

Timing of India-Asia collision: Geological, biostratigraphic, and palaeomagnetic constraints

Yani Najman,¹ Erwin Appel,² Marcelle Boudagher-Fadel,³ Paul Bown,³ Andy Carter,³ Eduardo Garzanti,⁴ Laurent Godin,⁵ Jingtai Han,⁶ Ursina Liebke,² Grahame Oliver,⁷ Randy Parrish,⁸ and Giovanni Vezzoli⁴

Received 28 April 2010; revised 18 July 2010; accepted 29 July 2010; published 21 December 2010.

[1] A range of ages have been proposed for the timing of India-Asia collision; the range to some extent reflects different definitions of collision and methods used to date it. In this paper we discuss three approaches that have been used to constrain the time of collision: the time of cessation of marine facies, the time of the first arrival of Asian detritus on the Indian plate, and the determination of the relative positions of India and Asia through time. In the Qumiba sedimentary section located south of the Yarlung Tsangpo suture in Tibet, a previous work has dated marine facies at middle to late Eocene, by far the youngest marine sediments recorded in the region. By contrast, our biostratigraphic data indicate the youngest marine facies preserved at this locality are 50.6–52.8 Ma, in broad agreement with the timing of cessation of marine facies elsewhere throughout the region. Double dating of detrital zircons from this formation, by U-Pb and fission track methods, indicates an Asian contribution to the rocks thus documenting the time of arrival of Asian material onto the Indian plate at this time and hence constraining the time of India-Asia collision. Our reconstruction of the positions of India and Asia by using a compilation of published palaeomagnetic data indicates initial contact between the continents in the early Eocene. We conclude the paper with a discussion on the viability of a recent assertion that collision between India and Asia could not have occurred prior to ~35 Ma.

Citation: Najman, Y., et al. (2010), Timing of India-Asia collision: Geological, biostratigraphic, and palaeomagnetic constraints, *J. Geophys. Res.*, 115, B12416, doi:10.1029/2010JB007673.

1. Introduction

[2] Precise determination of the timing and diachronicity of closure of Tethys and subsequent India-Asia collision and Himalayan evolution, is critical to accurate calculation of crustal shortening, required for models of accommodation of convergence. It is also important for the testing of hypotheses which link Himalayan orogenesis with global cooling [Raymo and Ruddiman, 1988] and changes in marine geochemistry [Richter et al., 1992]. While the most commonly quoted age of collision lies between 55 and 50 Ma,

published ages span ~65 to 34 Ma, with this range explained to some extent by different definitions and indicators of “collision” in an ongoing process. To quote but a few examples, Jaeger et al. [1989] suggested a ca 65 Ma age of collision based on the appearance of Asian fauna in India at this time. Klootwijk et al. [1992] recorded a distinct reduction in the velocity of northward drift of the Indian plate at 55 Ma, based on palaeomagnetic evidence. This they attributed to final suturing between India and Asia, with earlier variations ascribed to initial India-Asia contact as early as the Cretaceous-Tertiary boundary. Dating of eclogites by de Sigoyer et al. [2000] can be interpreted as due to continental subduction at ca 55 Ma, with continental collision interpreted at ca 47 Ma from the decreased rate of their exhumation at this time. Aitchison et al. [2007] propose a ~34 Ma age for collision based on their plate reconstructions of the relative positions of India and Asia through time, as well as additional lines of evidence (see section 5 for further discussion).

[3] Cessation of marine facies and the first arrival of Asian detritus on the Indian plate provide constraint to the minimum age of collision since seaways may persist on continental crust after initial contact between two plates has taken place, and there may be a considerable lag time between initial contact and sufficient build up of topography to supply

¹Lancaster Environment Centre, University of Lancaster, Lancaster, United Kingdom.

²Institut für Geowissenschaften Sigwartstrasse, University of Tuebingen, Tuebingen, Germany.

³Department of Geological Sciences, UCL, London, United Kingdom.

⁴Dipartimento di Scienze Geologiche e Geotecnologie, University of Milano-Bicocca, Milan, Italy.

⁵Department of Geological Sciences, Queen’s University at Kingston, Kingston, Ontario, Canada.

⁶Department of Geology, CAS, Beijing, China.

⁷School of Geography and Geosciences, University of St Andrews, St Andrews, United Kingdom.

⁸NIGL, BGS Keyworth, Nottingham, United Kingdom.

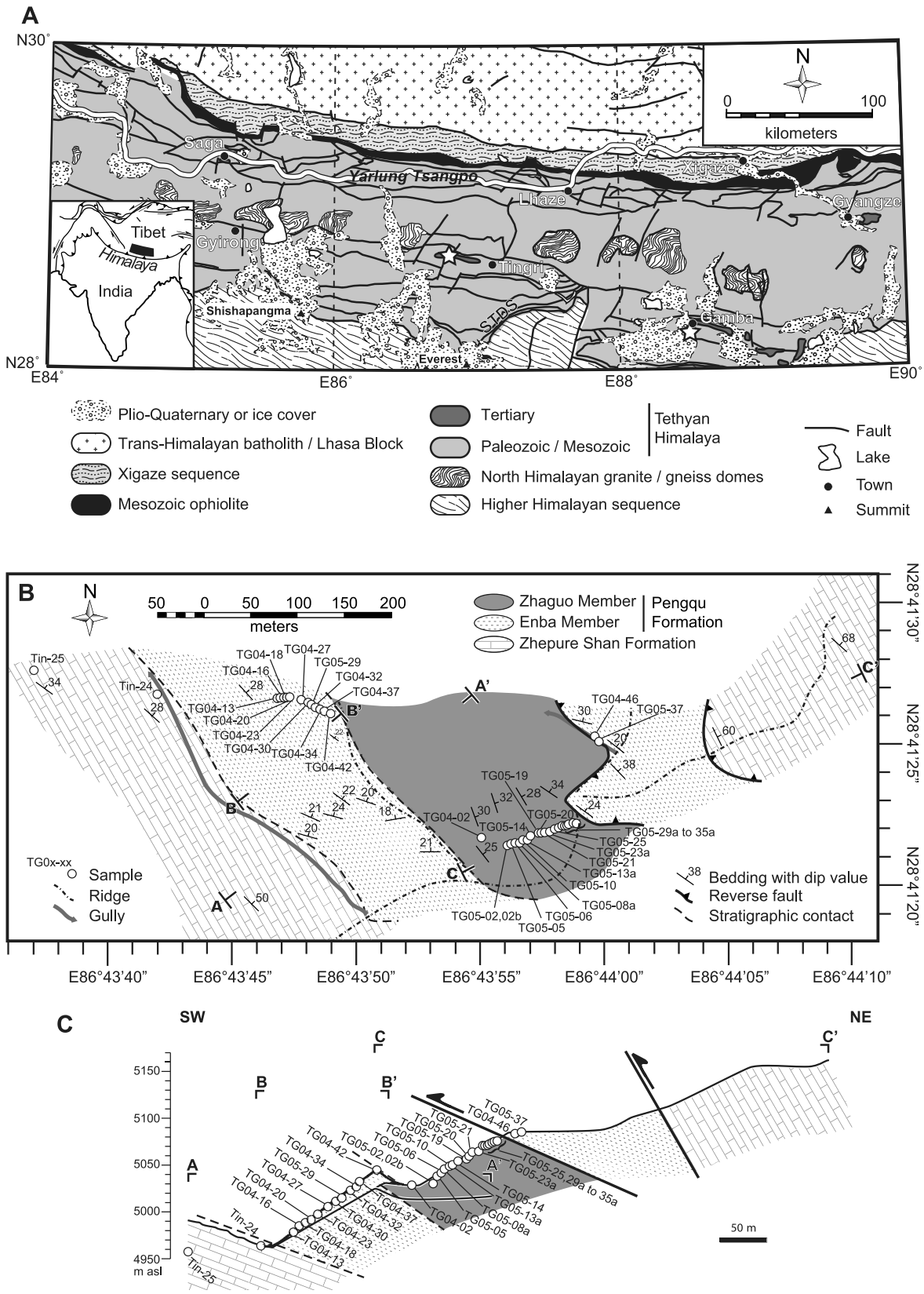


Figure 2. (a) Regional geological map of southern Tibet. Locations of the sections studied in previous and current research are shown by stars: the Qumiba and Gongza sections at Tingri and the Gamba section. Map adapted from *Larson et al.* [2010]. (b and c) Geological map and cross section of the Qumiba section. Locations of all samples analyzed for biostratigraphy, illite crystallinity, petrography, zircon U-Pb and fission track, and apatite fission track are shown.

and the Enba Member is conformable, and the contact between the Enba and Zhaguo members are disconformable. However, these researchers debate the temporal extent of the disconformity between the Enba and Zhaguo members, and their age and facies interpretations.

[7] Wang *et al.* [2002] consider the Pengqu Formation to be entirely marine. They date the base of the Enba Member as Zone NP15 (Lutetian) and the uppermost Enba Member as Zones NP16–17 (Lutetian–Bartonian). They consider the overlying Zhaguo Member to be of Zones NP18–20 age (Priabonian). They note a stratigraphically mixed assemblage indicating significant reworking at the Enba-Zhaguo boundary, and they consider the contact to be disconformable but with no significant hiatus, based on their biostratigraphy. By contrast, Zhu *et al.* [2005] consider the Enba Member to be marine facies of Zone P8 (50.6 Ma). They consider the overlying Zhaguo Member to be continental, based on their observations of facies and sedimentary structures. They therefore consider the fauna recorded by Wang *et al.* in the Zhaguo Member to be reworked. Zhu *et al.* reported a 4.25m regolith and paleoverisol at the Enba-Zhaguo contact which they consider to be further evidence of a disconformable contact. Thus, in their view, the red beds of the Zhaguo Member may be considerably younger than the Enba Member.

[8] Based on our geological mapping, we interpret the contacts between the Zephure Shan limestones and the overlying Enba Member, and between the Enba and overlying Zhaguo members as depositional. Although the actual Zephure Shan-Enba and Enba-Zhaguo contacts are not exposed (unlike Zhu *et al.* [2006], we did not trench to find the Enba-Zhaguo contact), the absence of any deformational features (fracturing, faulting, pressure solution) and the near-parallel nature of the beds of all three units indicate contacts are not structural. The minor dip differences between the Zephure Shan Formation and the Enba Member ($<10^\circ$), and between the Enba Member and the Zhaguo Member ($\approx 11^\circ$) may indicate the presence of two subtle angular unconformities. The top of the Zhaguo Member is truncated by a reverse fault, with Enba Member carried southward in the hanging wall. The clastic succession is truncated by overthrust Zephure Shan limestones (Figures 2b and 2c).

3. Biostratigraphy of the Qumiba Section

[9] We sampled from the Zephure Shan and Pengqu formations for biostratigraphic determination of age. All samples used can be located in Figure 2, and from the grid reference and altitude coordinates given in Table S1. Foraminifera from three limestone samples, two from the Zephure Shan Formation and one from the Enba Member, were identified from thin sections. Calcareous nannofossils from Enba and Zhaguo Member mudstones were analyzed using simple smear slides and standard light microscope techniques [Bown and Young, 1998]. Full analytical methodology is given in Text S1. Abundance and preservation categories as well as a complete taxonomic list for foraminifera and nannofossils are given in Text S2 and Figure S2.

3.1. Age of the Zephure Shan Formation

[10] We carried out biostratigraphic analysis from thin sections of two limestone samples from the Zephure Shan

Formation. Samples TIN24 and TIN25 were packed with nummulitic larger benthic foraminifera. The assemblages were randomly deposited and cemented with micrite. The presence of the larger benthic foraminifera *Assilina leymeriei*, *Discocyclina dispansa*, *Assilina* sp., *Nummulites atacicus*, *Assilina globosa* and *Discocyclina* sp., illustrated in Figure 3, indicate an early Eocene age, (shallow benthic zone SBZ 8; ~ 53 –54 Ma). Planktonic foraminifera were rare and mainly consisted of *Globigerina* spp. However, the presence of *Planorotalites chapmani* corroborates an age not younger than early Ypresian (~ 54.5 –52.5; lowermost P7/P6, Planktonic Foraminifera Zone). The constant presence of planktonic foraminifera within the benthic assemblages indicates an open marine fore-reef environment. Our larger benthic foraminifera data agree with the Ypresian age determination of Zhu *et al.* [2005] but not with the younger Lutetian age of Wang *et al.* [2002] (Figure 1).

3.2. Age of the Enba and Zhaguo Members

[11] We found no difference between the calcareous nannofossil assemblages preserved in the Enba and Zhaguo members and therefore consider them together. All samples host stratigraphically mixed nannofossil assemblages, typically with approximately 50% Late Cretaceous and 50% early Paleogene components. Identifying discrete assemblage ages within this mix is problematic, however, there do appear to be coherent Cenomanian (*Corollithion kennedyi*, *Axopodorhabdus albianus*, *Helenea chianstia*, *Rhagodiscus achlyostaurion*), Campanian (*Uniplanarius trifidus*), Maastrichtian (*Micula murus*), mid-Paleocene (*Fasciculithus pileatus*, *F. ullii*, *F. bitectus*), and Paleocene/Eocene boundary interval (*Calciosolenia aperta*, *Discoaster multiradiatus*, *Fasciculithus involutus*) elements. The dominant nannofossils are consistently *Coccolithus pelagicus* (Cenozoic), *Toweius pertusus* (Paleocene–lower Eocene) and *Watznaueria barnesiae* (Mesozoic). The youngest assemblage components, which may represent the depositional age of these sediments, are always rare but nevertheless age diagnostic, and comprise spinose sphenoliths (*Sphenolithus conspicuus*, *S. radians*, *S. villae*), *Tribrachiatus orthostylus* and *Discoaster kuepperi*. These species are compatible with an age corresponding to nannofossil Zones NP11–12 (Ypresian, 50.6–53.5 Ma) (see, for example, stratigraphic ranges documented by Perch-Nielsen [1985] and Bralower and Mutterlose [1995]). The minimum age of NP12 (50.6–52.8 Ma) is supported by the absence of reticulofenestrads (i.e., *Reticulofenestra*, *Dictyococcites* and *Cyclicargolithus*), which became the dominant Paleogene coccoliths after their appearance in this zone, and strongly indicates that there are no younger nannofossils in these sediments. Selected nannofossils are illustrated in Figure 4.

[12] We also analyzed one sample (TG04–32D; several thin sections) from the Enba Member which yielded abundant planktonic foraminifers that indicate a similar stratigraphic age to the nannofossils. Again these assemblages have stratigraphically mixed elements, including reworked Late Cretaceous and Paleocene forms occurring in micritic or sparitic clasts appearing as patches in the matrix, together with early Eocene forms which we do not consider to be reworked considering their in situ occurrence in the sparitic matrix. The youngest age-diagnostic foraminifera are morozovellids (e.g., *Morozovella aragonensis*, *M. quetra*,

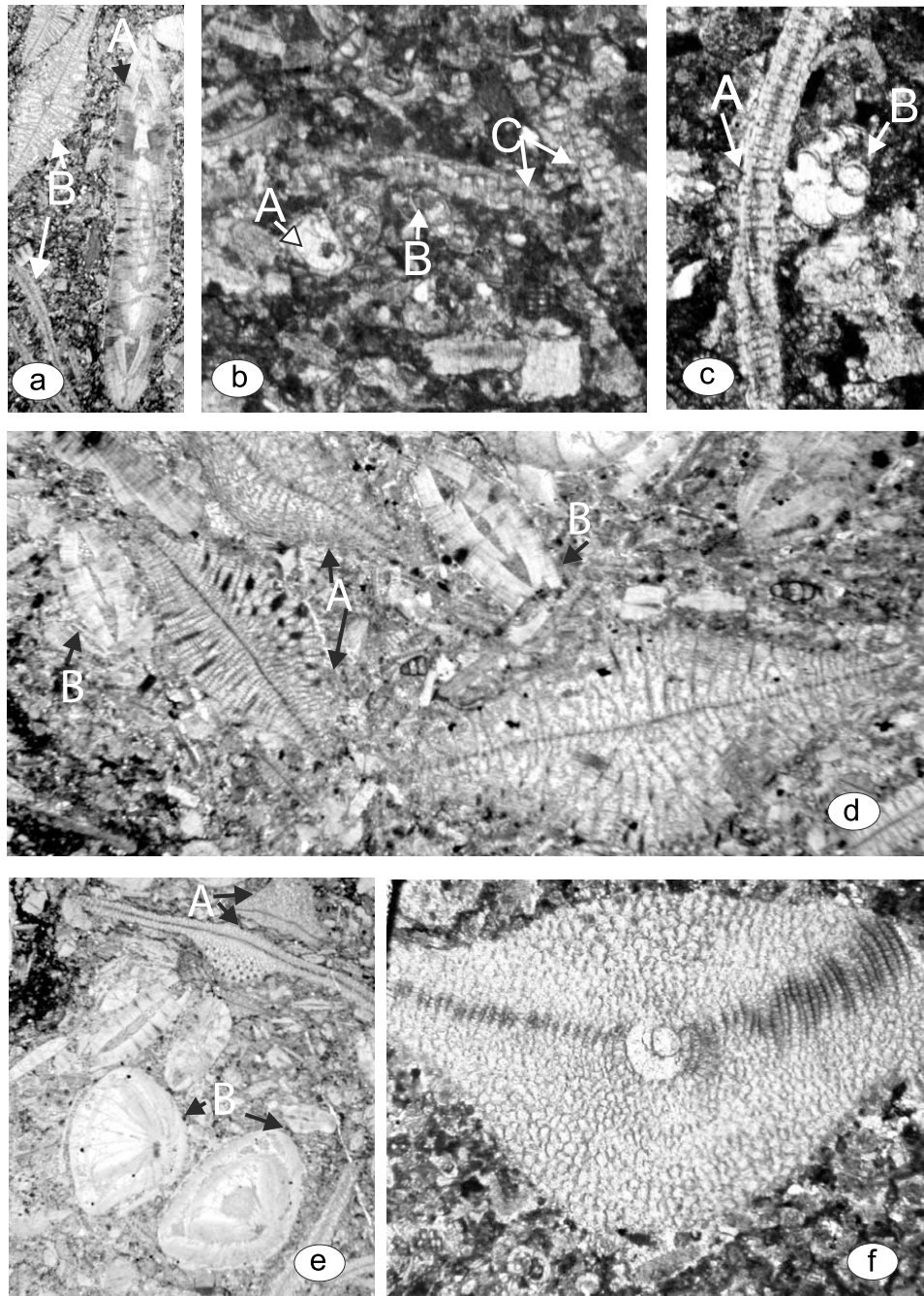


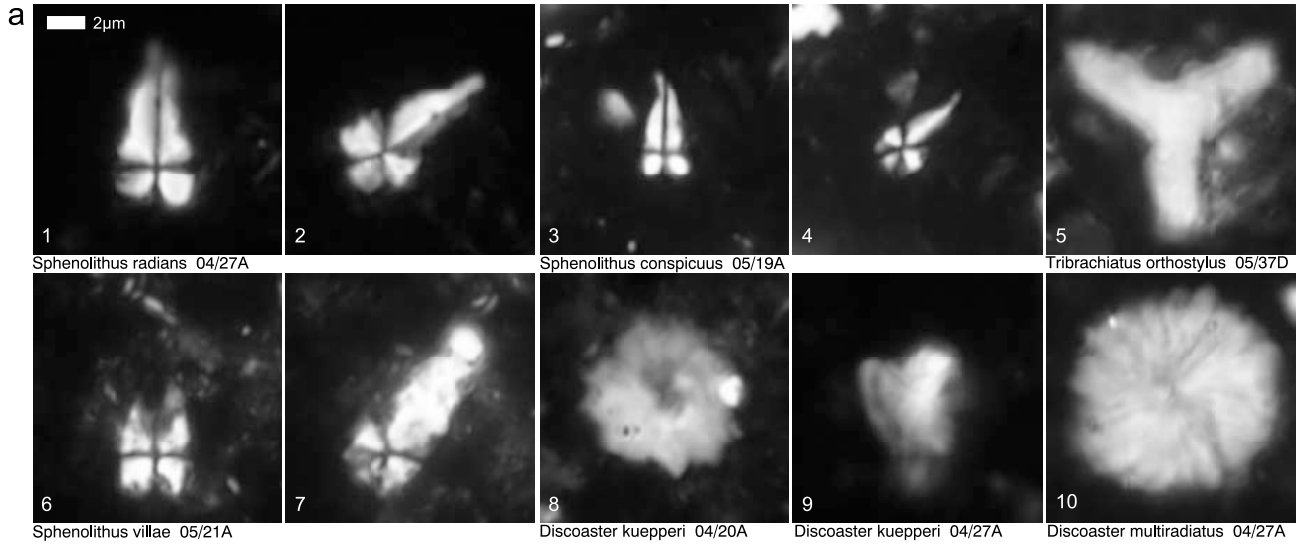
Figure 3. Foraminifera from the Zephure Shan Formation. All photos taken from sample slide TIN24. (a) A, *Assilina leymeriei* (d'Archiac and Haime); B, *Discocyclina dispansa* (Sowerby), 6X. (b) A, *Globigerina* sp.; B, *Planorotalites chapmani* (Parr); C, fragments of *Discocyclina* sp., 60X. (c) A, fragments of *Discocyclina* sp.; B, *Planorotalites chapmani* (Parr), 90X. (d) A, *Discocyclina dispansa* (Sowerby); B, *Assilina* sp., 19X. (e) *Nummulites atacicus* Leymerie, *Assilina globosa* (Leymerie), *Discocyclina* sp., 10X. (f) *Discocyclina dispansa* (Sowerby), 32X.

M. formosa, *M. lensiformis*) and acarininids, *Globigerina* spp., and *Globeriginatheka* sp.). The co-occurrence of these taxa indicates foraminiferal zones P7–8 (ca. 50.4–52.3 Ma). This is a stratigraphic match with our nannofossil zone assignment and comparable to the planktonic foraminifera previously reported from the Enba Member by Zhu *et al.* [2005]. Fauna are illustrated in Figure 4.

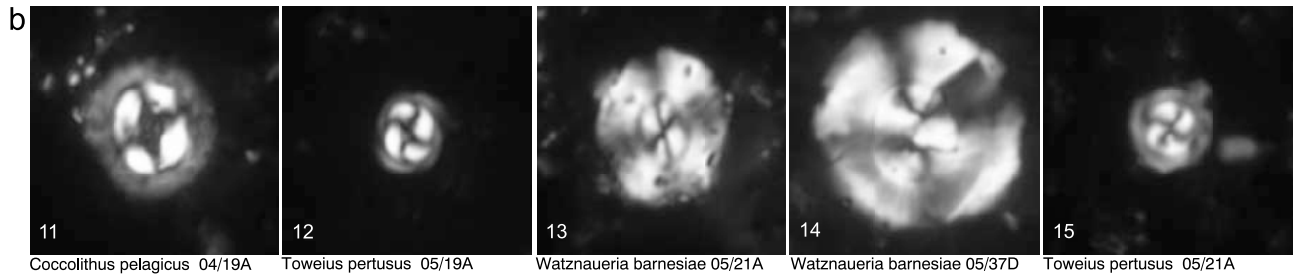
3.3. Comparison With Data Along Strike

[13] There is little precise age dating of the youngest marine facies of sections in the near vicinity to the Qumiba section. In the Gamba region (Figures 1 and 2a), the Zongpu Formation Indian Tethyan margin limestones dated biostratigraphically at middle Paleocene to early Eocene age are overlain by the Zongpubei Formation consisting of green marls, oolitic

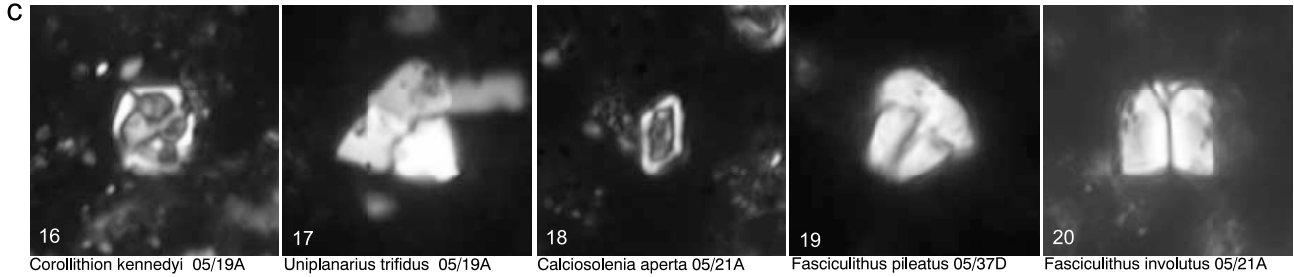
YOUNGEST AGE-DIAGNOSTIC NANNOFOSSIL TAXA



DOMINANT NANNOFOSSIL TAXA



SELECTED REWORKED NANNOFOSSIL TAXA



SELECTED PLANKTONIC FORAMINIFERA

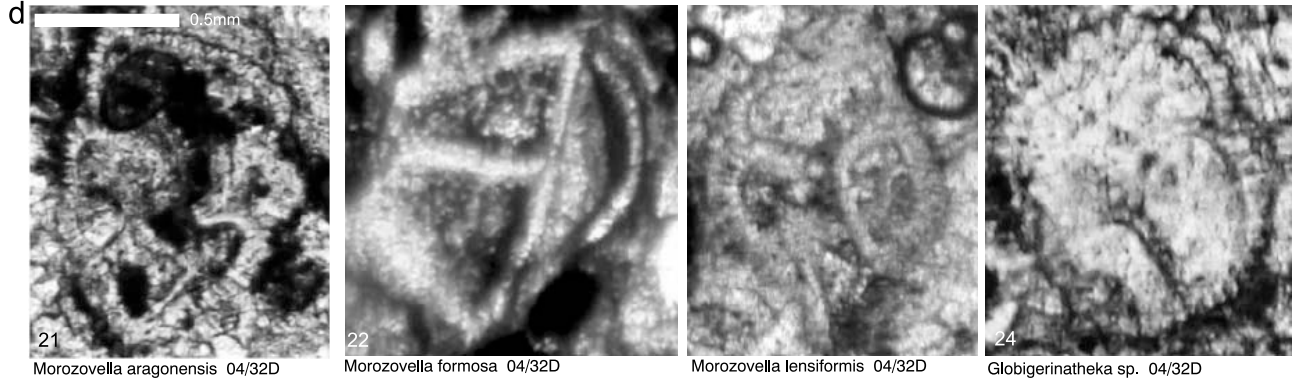


Figure 4. Fauna from the Pengqu Formation. Images of selected nannofossil taxa, including (a) age diagnostic forms, (b) the dominant species, and (c) conspicuous reworked Cretaceous taxa. Unlabelled images are the same specimen in different orientation. (d) Planktonic foraminifera from sample TG04–32D, Enba Member: *Morozovella aragonensis* (Nuttall), 40X, *Morozovella formosa* (Bolli), 40X, *Morozovella lensiformis* (Subbotina), 45X, and *Globigerinatheka* sp., 50X.

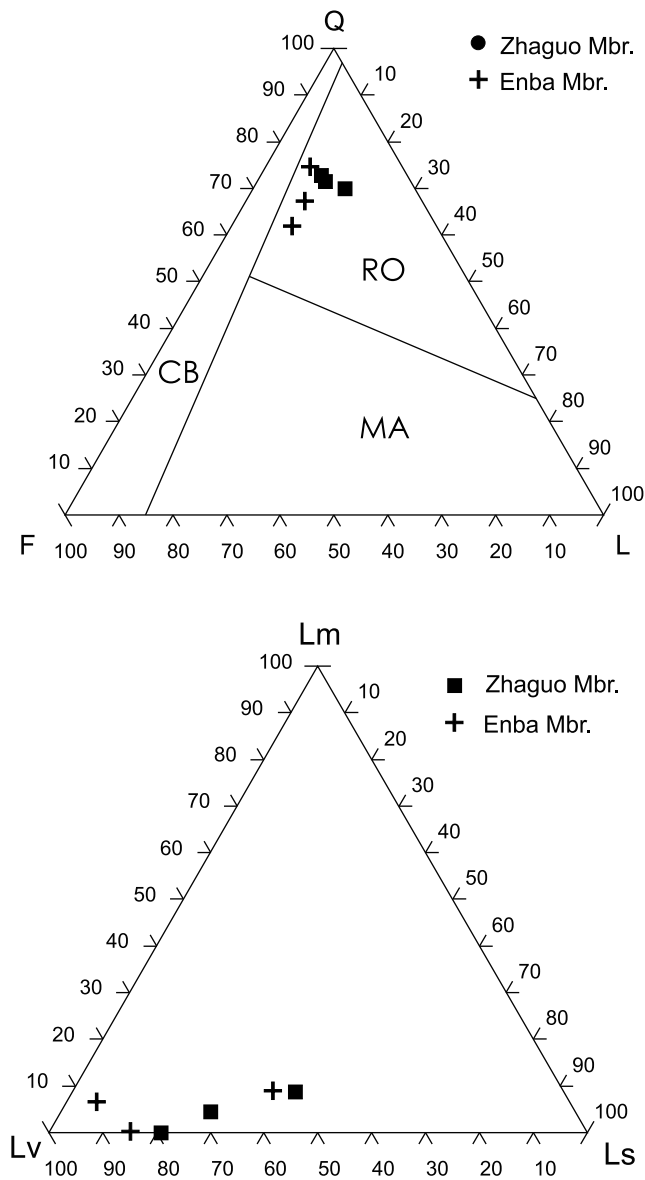


Figure 5. Petrography of the Enba and Zhaguo members. QFL plot, apices: Q, quartz; F, feldspar; L, lithics. Fields, after Dickinson [1985]: RO, recycled orogen; CB, continental block; MA, magmatic arc. Lithics plot, apices: Lv, volcanic lithic fragments; Ls, sedimentary lithic fragments; Lm, metamorphic lithic fragments.

limestones containing *Ostrea*, red clays, siltstones and rare sandstones, of marginal marine facies. Since no age-diagnostic fossils are found in the Zongpubei Formation, Willems and Zhang [1993a] assigned an early Eocene age to the formation, based solely on its stratigraphic position above the Zongpu Formation. In the Gongza section near Tingri (Figures 1 and 2a), Willems and Zhang [1993b] and Willems *et al.* [1996] record green marls and overlying continental red beds in faulted contact with the underlying passive margin limestones of the Zephure Shan Formation, which they biostratigraphically dated as extending to Lutetian (but note that Blondeau *et al.* [1986] date the formation as extending only to early Eocene). Based on similar stratigraphy and facies, Willems and Zhang correlate the overlying marls and

red beds with the Zongpubei Formation at Gamba. They assign them a Lutetian or younger age based on (1) the (disputed) [Blondeau *et al.*, 1986] age of the Zephure Shan Formation in faulted contact below and (2) the (disputed) [Zhu *et al.*, 2005] correlation with the facies at Gamba, which are also unfossiliferous and dated only by their stratigraphic position above the passive margin limestones.

[14] Further along strike in India, final recorded marine sedimentation is more precisely dated. The Nummulitic limestones represent the youngest preserved marine sedimentary rocks documented in the suture zone and the Kong Formation represents the youngest marine sedimentary rocks preserved to the south in the Tethys Himalaya (Figure 1). At no location has marine sedimentation been dated any younger than 50.5 Ma [Critelli and Garzanti, 1994; Fuchs and Willems, 1990; Green *et al.*, 2008; Henderson *et al.*, 2010; Najman *et al.*, 2010; Nicora *et al.*, 1987;] comparable with our data from the Qumiba section in Tibet.

4. Provenance of the Rocks of the Qumiba Section, Tibet

[15] When the Tethys Ocean closed, the Palaeozoic–earliest Cenozoic Tethyan sediments of the northern Indian passive continental margin collided with the Andean-type southern active margin of Asia, represented by the Mesozoic–Paleogene batholiths of the Trans-Himalaya, along what is now termed the Indus/Yarlung-Tsangpo suture zone (Figure 2a). Thus, the arrival of Asian continental arc-derived detritus onto the Indian plate provides a minimum time of collision. The provenance study below discriminates between Indian versus Asian plate detritus in the Pengqu Formation using (1) petrography to identify metamorphic and sedimentary detritus of the Indian plate versus igneous detritus of the Asian plate and (2) zircon mineral dating, since grains of earliest Tertiary–Mesozoic U–Pb age are diagnostic of derivation from the Asian plate, as discussed further in the following sections.

4.1. Petrography: Methods and Results

[16] The six analyzed samples are very fine grained sandstones (average median diameter $3.7 \pm 0.3 \phi$; grain size determined by visual comparison and direct measurement in thin section). Replacement by authigenic carbonate occurs in all samples ($9 \pm 4\%$ of the rock), as well as interstitial phyllosilicate grown during diagenesis ($5 \pm 3\%$ of the rock). In each sample, 400 points were counted by the Gazzi-Dickinson method [Dickinson, 1985]. Traditional ternary parameters and plots (QFL, LmLvLs) [Ingersoll *et al.*, 1993] were supplemented, specifically where lithic grains are concerned, by an extended spectrum of key indices [Garzanti and Vezzoli, 2003]. Results are illustrated in Figure 5 and tabulated in Table S2.

[17] Detrital modes of Enba and Zhaguo sandstones do not show marked differences, and consequently are discussed jointly. Composition is quartzofeldspathic, but with significant felsitic and microlitic volcanic rock fragments, and subordinate sedimentary (sparite, micrite, shale, chert) and metamorphic (shale, phyllite, quartz-mica, chloritoschist, possibly rare serpentinite) grains. Volcanic detritus is more felsic in Zhaguo sandstones, where monocrystalline quartz and nonvolcanic lithic grains tend to increase slightly with

respect to Enba sandstones. A very poor heavy-mineral assemblage, strongly affected by diagenetic dissolution, consists exclusively of ultrastable species (zircon, tourmaline, rare rutile and chrome spinel) with no amphibole or pyroxene. Micas are rare. Reworked specimens of *Globotruncana* are frequently observed.

[18] Bulk petrography ($Q\ 69 \pm 4$, $F\ 18 \pm 5$, $L_v\ 8 \pm 2$, $L_s\ 2 \pm 1$, $L_m\ 3 \pm 1$; $P/F\ 58 \pm 7$), in particular the notable proportion of volcanic lithics and plagioclase, indicates significant contribution from a magmatic arc. However, the composition has a much more quartzose mode than found in modern arc settings [Garzanti et al., 2007; Marsaglia and Ingersoll, 1992]. Significant dilution by detritus derived from a quartzose sedimentary source is thus indicated, with dissolution of unstable grains in the wet subequatorial climate (as evidenced from palaeomagnetic data (section 5.1) and presence of kaolinite (section 4.2.1)) also likely to have influenced the resulting mode. The Enba and Zhaguo sandstones therefore display mixed provenance. Quantitative provenance analysis carried out by end-member calculations using a linear mixing model [Weltje, 1997] indicate provenance from the volcanic cover (at least 10–15% of the total detritus, including volcanic rock fragments and fragments of plagioclase grains) and batholithic plutonic roots of a partly dissected magmatic arc (at least 20–25% of total detritus, including much plagioclase and K-feldspar), with the remainder derived from recycling of a sedimentary succession including quartzose sandstones.

[19] Our data are broadly consistent with previous petrographic work by Zhu et al. [2005]. The much greater proportion of micrite/spirite grains and interstitial matrix reported by Zhu et al. may be ascribed to different criteria in evaluating diagenetic replacements and interstitial phyllosilicate growth at the expense of framework grains in very fine grained sandstone samples.

4.2. Mineral Dating: Methods and Results

4.2.1. Burial Temperatures Determined From Clay Mineralogy and Illite Crystallinity Data

[20] In order to determine if the mineral ages reflect the timing of cooling in the source region, or the time of post-depositional resetting if minerals have been subjected to temperatures above their closure temperature subsequent to burial, the degree of postdepositional heating that the host rock has been subjected to needs to be determined. The thickness of illite crystals is dependent on metamorphic grade [Weber, 1972]. Thus, XRD analyses on the $<2\mu$ (diagenetic) fraction of rocks, to determine illite crystallinity as well as clay mineralogy (which is also diagnostic of metamorphic grade), enable postdepositional burial temperatures of the

rocks to be determined. Eighteen Enba Member mudstones/siltstones and 25 Zhaguo Member samples were analyzed. Analytical methodology is given in Text S1.

[21] All samples contained mixed layer illite-smectite clays and chlorite. Additionally, the Enba Member contained kaolinite. This clay mineralogy is distinctive of the diagenetic zone of burial. Hb_{rel} values are >700 for the Zhaguo Member, and >600 for the Enba Member (with one sample at 391), indicating diagenetic facies ($<200^\circ\text{C}$) which has Hb_{rel} values >278 [Blenkinsop, 1988]. Since the partial annealing zone for fission tracks in zircon lies between $\sim 200\text{--}320^\circ\text{C}$ [Tagami et al., 1998], we consider that our zircon fission track ages, given below, represent the timing of cooling and exhumation in the source region. The U-Pb isotopic system in zircons is unperturbed by temperatures commensurate with sedimentary rocks. All data are given in Table S3.

4.2.2. Dating of Detrital Zircons by U-Pb and Fission Track Techniques

[22] Four samples, two from the Enba Member and two from the Zhaguo Member, were counted for zircon fission track analysis. Two samples, one from the Zhaguo Member and one from the Enba Member were chosen for U-Pb dating of zircons, and one sample was chosen for double dating of the grains by both techniques. Full analytical methodologies are given in Text S1.

[23] In both the Enba and Zhaguo members, the majority of grains have U-Pb ages between Cretaceous–earliest Eocene (140–55 Ma) with uncommon grains > 500 Ma (Figure 6 and Table S4). Zircon fission track ages are also dominantly Cretaceous–earliest Eocene, with older ages spanning back through the Mesozoic (Figure 7 and Table S5). The majority of grains analyzed by both techniques have similar U-Pb and zircon fission track (ZFT) ages, illustrated by their position close to the 1:1 line on the U-Pb versus ZFT plot (Figure 8 and Table S6). These are interpreted as formation ages from an igneous source. The grains with Precambrian U-Pb ages were exhumed from depth during the Mesozoic.

[24] We also carried out apatite fission track dating on three samples (see Table S5 for data and brief discussion). Since apatite has a relatively low partial annealing zone, these data do not contribute to provenance determination since the ages do not unequivocally represent the timing of cooling in the source area rather than the time of postdepositional cooling following diagenesis in the basin.

4.3. Interpretation: Provenance of the Pengqu Formation

[25] Given the location of the Enba and Zhaguo members, a southern source from the Indian plate versus a north-

Figure 6. Histograms with overlain probability density plots of $^{206}\text{U}/^{238}\text{Pb}$ ages of detrital zircons from the Enba (TG04–18A) and Zhaguo (TG04–2A) formations, compared to the ages of zircons from the potential source regions of the Indian plate (Tethyan Himalaya) and Asian plate (southern Trans-Himalaya). (left) Data are plotted at 2 sigma error, histogram bin width 25 Myr. (right) Corresponding subsets of each data set, in the range 0–200 Ma and enlarged (bin width 10 Myr). Asian plate data represent analyses from the southern Gangdese batholiths, excluding data from the northern range as defined by Wen et al. [2008], since the southern slopes are the most likely source region to the suture zone. Data are therefore compiled from Wen et al. [2008] and references therein [Booth et al., 2004; Harrison et al., 2000; McDermid et al., 2002; Miller et al., 1999; Mo et al., 2005; Quidelleur et al., 1997; Scharer et al., 1984]. Indian plate data are taken from the compilation published in Gehrels et al. [2008]. The population of zircons aged 200–400 Ma discovered by Aikman et al. [2008] is not included in this synthesis due to uncertainty over the terrane assignment of their host rock [see Aikman et al., 2008, and references therein], and their omission does not change our interpretation. Grains >1700 Ma were not found in the Enba or Zhaguo members and are excluded from the Indian and Asian plate plots.

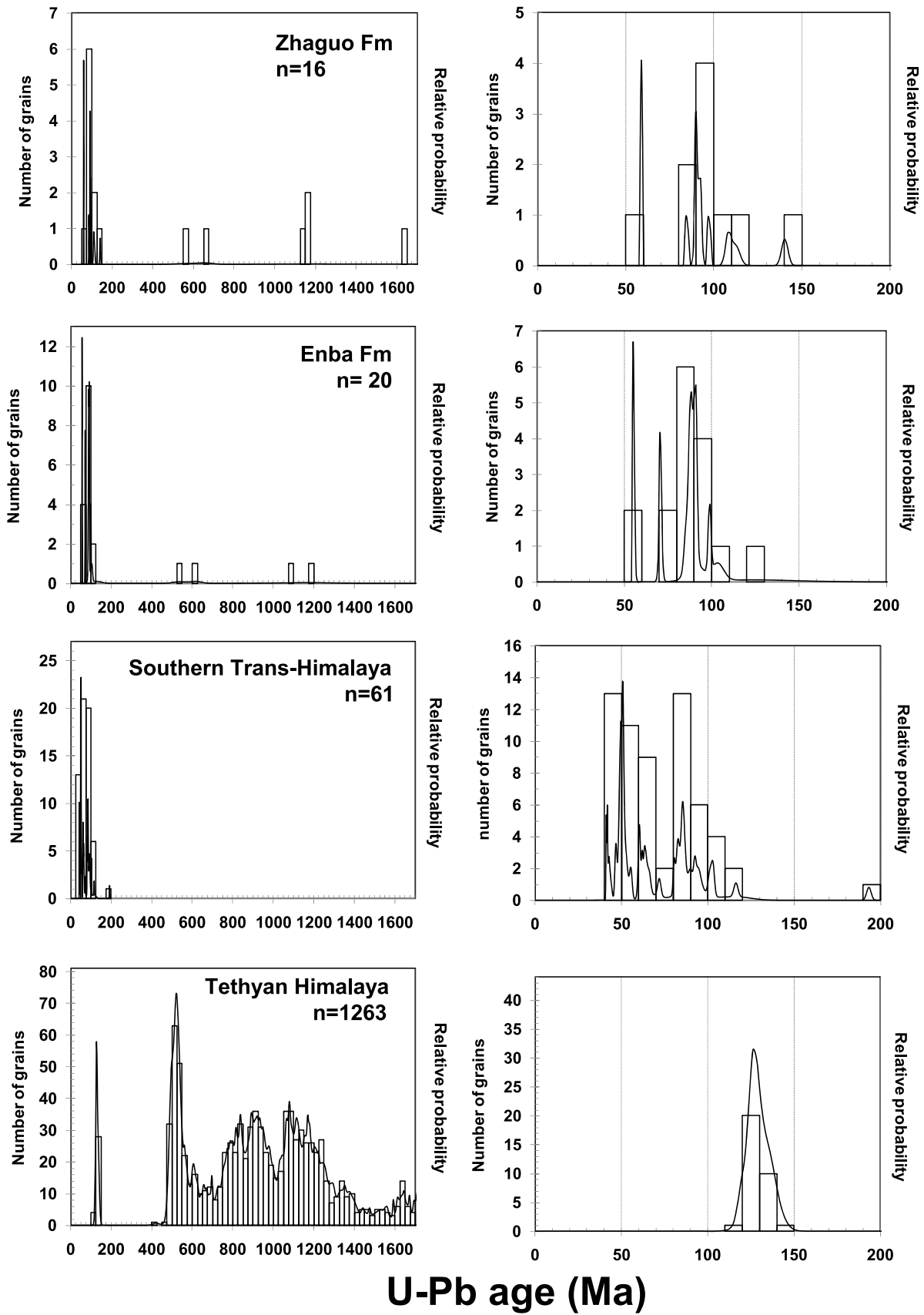
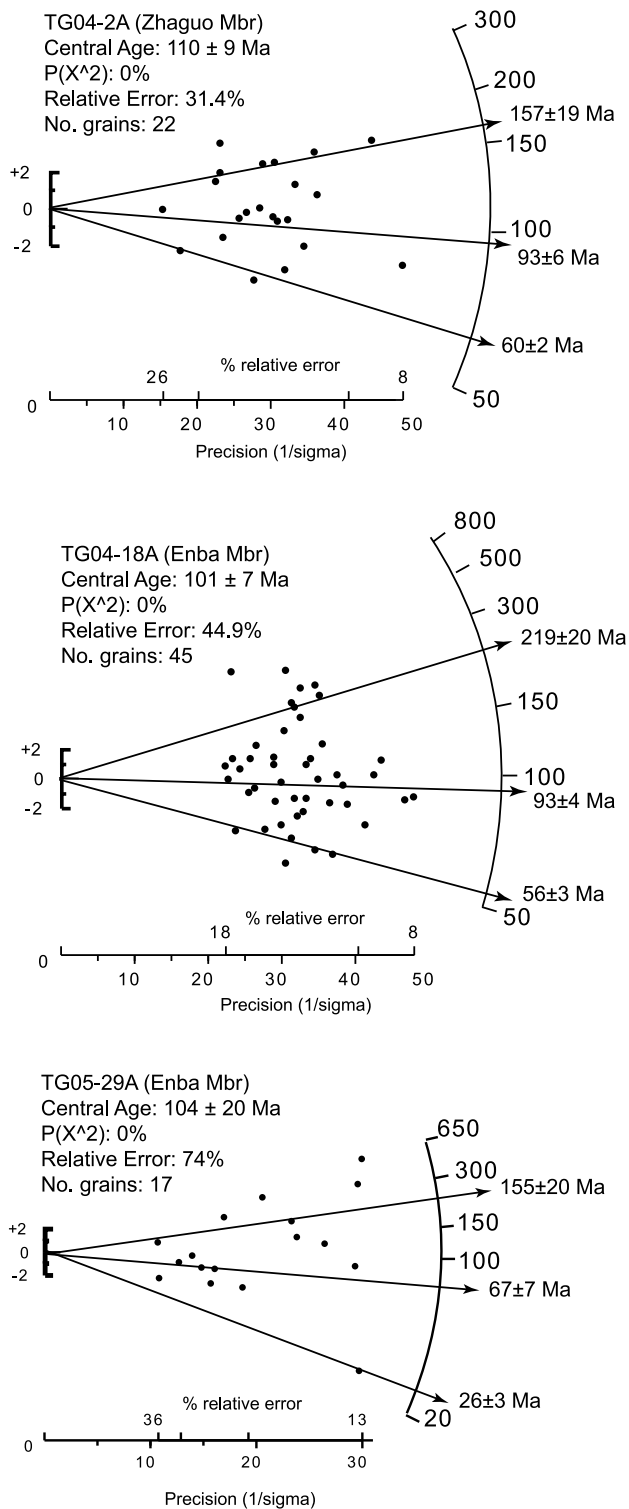


Figure 6



TG05-2B (Zhaguo Mbr) consists only of 4 grains, dated as one population at 102.5 ± 19.8 Ma.

Figure 7. Radial plots of zircon fission track (FT) data showing the principal age modes extracted using the method of *Galbraith and Green* [1990]. The size of each data set is lower than desirable due to the relative sparsity of zircon grains suitable for FT analysis.

ern source from the Asian plate needs to be considered (Figure 2a). As summarized above, the southern margin of the Asian plate consists of a Mesozoic-Paleogene Andean-style batholith of the Trans-Himalayan continental arc intruded through Precambrian basement and overlying Phanerozoic sedimentary rocks of the Asian plate Lhasa Block. The northern margin of the Indian plate consists of Paleozoic-Cretaceous passive margin sedimentary rocks of the Tethyan Himalaya, with rocks of the Higher Himalaya, metamorphosed to medium-high grade during the Tertiary Himalayan orogeny, located to the south [*Hodges, 2000*, and references therein].

[26] Our petrographic, U-Pb and fission track (FT) zircon data provide evidence for a consistent interpretation of provenance. By comparison of U-Pb ages of zircons from the Enba and Zhaguo members with zircons from the Trans-Himalayan arc and Tethyan Himalaya (Figure 6) it can be seen that the majority of Enba and Zhaguo Member grains (dated Cretaceous-earliest Eocene) are sourced from the Asian plate, where the Trans-Himalayan batholith provides a source with abundant zircons spanning this age range, in contrast to the Indian plate where such grains are uncommon (Figure 6, bottom two rows). Although there is a peak of Early Cretaceous ages recorded from the Wolong volcanics of the Indian plate [*Hu et al., 2009a*] (Figure 6) which could conceivably have contributed some grains to the sediments of the Pengqu Formation, we do not consider them a viable alternative source to the Trans-Himalaya since (1) the dominant age population in the Pengqu Formation is younger than the restricted range of the Wolong volcanics, and (2) Cretaceous grains make up between 3 and 28% of zircons in the Wolong volcanics, the rest of the grains being of Cambro-Ordovician and older age. Given this low proportion of Cretaceous-aged grains in the unit, and the relatively restricted exposure of this unit compared to the Precambrian-aged zircon bearing Tethyan Himalaya as a whole, it seems highly improbable that the dominant population of Palaeogene-Cretaceous grains in the Pengqu Formation could be sourced from this unit.

[27] Fission track data show that these grains have Cretaceous-Paleocene fission track ages, with individual grain ages similar to the grain's U-Pb age, typical of grains of igneous origin (Figure 8). Fission track ages from all samples are exclusively Mesozoic and younger (Figure 7). This is consistent with an Asian source, but inconsistent with Indian derivation, since Paleozoic grains make up a significant proportion of the population eroded from the Indian plate during the Eocene [*Jain et al., 2009; Najman et al., 2005*].

[28] The grains with U-Pb ages >500 Ma may be recycled from sedimentary rocks of either the Indian plate or the Asian plate Lhasa Block, both of which contain zircons of Precambrian age [e.g., *Chu et al., 2006; Gehrels et al., 2008; Leier et al., 2007*]. We speculate that the Lhasa Block could be the more likely source for these grains in view of these grains' Mesozoic zircon fission track ages (Figure 7). While the Lhasa Block was undergoing crustal thickening and exhumation subsequent to collision with the Qiangtang terrain to the north during the Late Jurassic-Early Cretaceous [*Kapp et al., 2005*], thrusting began only later on the Indian plate margin; not before the latest Cretaceous at the earliest [*Searle et al., 1988*]. A mixed arc and recycled sedimentary

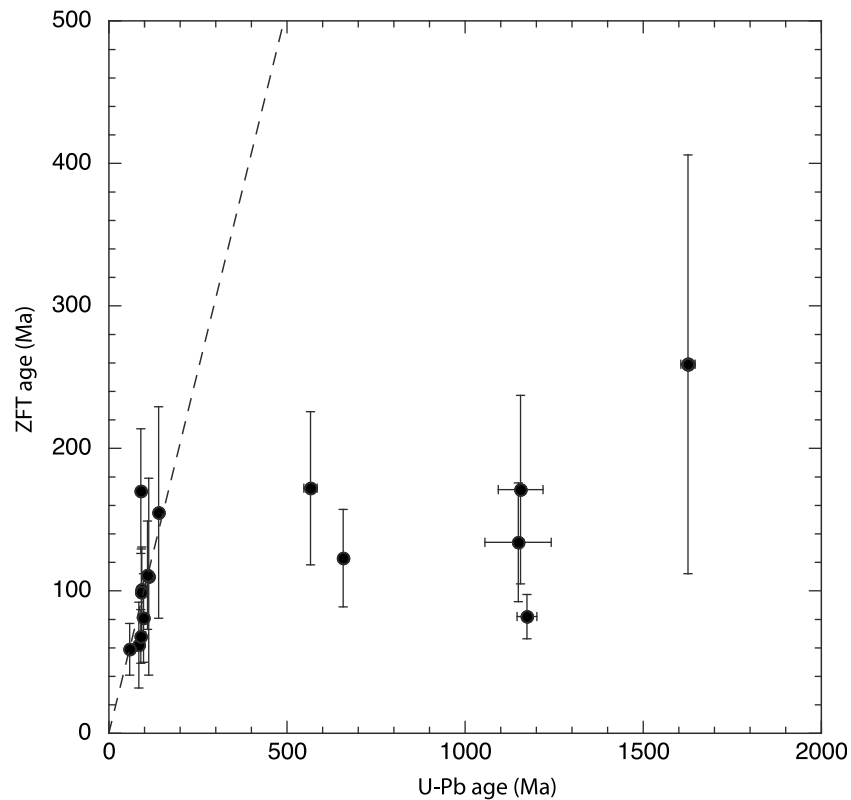


Figure 8. U-Pb versus zircon fission track (ZFT) ages for double dated zircon grains in sample TG04–2A Zhaguo Member. Both U-Pb and ZFT ages were quoted at 2 sigma errors. Dashed line shows the 1:1 correlation where ZFT age = U-Pb age. One grain has an apparent ZFT age that is older than its U-Pb age. We attribute this either to bad counting or to misidentification of the correct ZFT-dated grain for U-Pb dating in the crowded mount.

source is consistent with our petrographic data (section 4.1) which shows derivation in part from volcanic covers and batholithic roots of a partly dissected magmatic arc and in part from recycling of a sedimentary succession including quartzose sandstones.

[29] Our data thus show evidence that Asian detritus was deposited on the Indian plate by 50 Ma thereby providing a minimum constraint to the time of collision. Mesozoic zircons are found in sediments dated at 55 Ma in the Zheba section in Tibet [Ding *et al.*, 2005], in line with the more northerly position of this section compared to the Qumiba locality, thereby providing further constraint to the time of India-Asia collision. Our provenance interpretation is not at variance with that of previous workers [Wang *et al.*, 2002; Zhu *et al.*, 2005] who considered that these Tertiary rocks of the Pengqu Formation show first evidence of erosion from suture zone ophiolites and continental arc rocks of the Asian margin based on the presence of volcanic lithic fragments and euhedral feldspars in the sandstones, composition of Cr-spinel, and sandstone and shale geochemistry, in addition to south directed palaeocurrent indicators. However, more recently, Aitchison *et al.* [2007] proposed that the detritus with such a signature was derived from an intraoceanic arc and ophiolite sequence, the combined Dazhuqu-Baigang-Zedong terrains, sandwiched between the Indian and Asian plate. More isotopic data need to be collected from this arc before a robust comparison of signatures between this arc

and Enba and Zhaguo formation detritus can be made, and it is certainly correct that some types of detritus, for example Cr-Spinel, could be consistent with such a source. However, at present, we consider the source, at least of the zircons with Cretaceous–earliest Eocene U-Pb ages, which comprise 72% of the detrital zircon population, to be more likely derived from the Trans-Himalayan batholith of the Asian plate, rather than the Dazhuqu-Baigang-Zedong intraoceanic arc and ophiolite, because U-Pb ages of zircons that have been dated from the intraoceanic arc indicate that it is late Jurassic or older [McDermid *et al.*, 2002]. Zircons of such age in the Enba and Zhaguo members are extremely rare, and while we acknowledge that our data set is small, the result of the time consuming nature of the double-dating technique, our data are similar to a much more comprehensive data set from the same rocks analyzed by Hu *et al.* [2009b]. Instead, zircons from the Enba and Zhaguo members are Cretaceous–earliest Eocene age, which is in agreement with the range of ages documented from bedrock data of the Trans-Himalayan batholith (Figure 6). The dominant population in the Enba and Zhaguo Formation is aged between ~85–105 Ma and mirrors a peak of ages between 110 and 80 Ma documented in the Trans-Himalayan batholith [Ji *et al.*, 2009; Wen *et al.*, 2008]. The lack of a clearly defined peak at ~50 Ma in the Enba and Zhaguo formations, which can be clearly seen in the batholiths signature (Figure 6) is explained when the depositional age of the sedimentary rocks is taken into account.

It should also be noted that if metamorphic ages (70–90 Ma) of amphibolites and blueschists within serpentinite-matrix melanges along the southern margin of the intraoceanic arc-ophiolite complex are interpreted as the time of the arc-ophiolite's obduction on to the Indian margin [Aitchison *et al.*, 2000] rather than subduction of a spreading center [Aitchison *et al.*, 2003], then the ages of the zircons recorded in the Enba and Zhaguo members extend younger than the time of proposed obduction onto the Indian plate.

5. Discussion: Do Existing Geological and Palaeomagnetic Constraints “Demand” India-Asia Collision Occurred “No Earlier Than the Oligocene”?

[30] Our provenance data from the Qumiba sedimentary succession provide evidence of collision by 50 Ma, determined from the first arrival of Asian material on the Indian plate at this location. However, Aitchison *et al.* [2007] attribute this detritus to erosion not from Asia, but from an intraoceanic arc and ophiolite (the Dazhuku, Bainang and Zedong terrains), a provenance interpretation that we do not favor, as discussed above. Aitchison *et al.* propose that it is this intraoceanic arc-India collision which occurred around ~55 Ma, and they consider that “...as the geological record and constraints on the relative positions of India and Asia demand, the continental collision occurred no earlier than the Oligocene....” Their lines of evidence are as follows.

[31] (1) Their determination of the relative positions of India and Asia during the early Cenozoic require that collision occurred at <35 Ma and the two continents were too far apart to have collided at 55 Ma.

[32] (2) They consider that the geological record shows that cessation of marine facies, the beginning of continental molasse sedimentation along the suture zone, onset of major regional sedimentation, cessation of continental subduction along the southern margin of Eurasia, and initiation of major collision-related thrusting occurred later than previously believed. We discuss these lines of evidence below.

5.1. Position of the Indian and Asian Plates During the Cretaceous–Earliest Cenozoic as Determined From Palaeomagnetic Data

[33] In Figure 9 we present a reconstruction of the paleogeographic configuration between 58.5 to 45 Ma based on available paleomagnetic data (Table 1). The southern margin of Eurasia (shaded area) is determined for a reference point at the Indus-Yarlung suture zone (IYSZ) (29°N/90°E) selected at a best mean longitude close to the sampling areas of the paleomagnetic data involved. The results in Figure 9 comprise new data from the Paleocene-Eocene Linzizong volcanic rocks in the Linzhou (mainly) and Namling basins and the Mendui area on the Lhasa Block. According to the nomenclature of Dong *et al.* [2005] three different formations can be distinguished; the paleolatitudes derived for these formations are shown in Figure 9 by blue lines. Only results from volcanic rocks are considered here. Paleolatitudes for the reference point yield 6.7°N for the Dianzhong Formation (Fm) (Linzhou and Namling [Chen *et al.*, 2010]), 11.6°N for the Nianbo Fm (Linzhou and Mendui [Chen *et al.*, 2010; Sun *et al.*, 2010]), 13.2°N for dykes intruded into the Nianbo Fm [Liebke *et al.*, 2010], and 16.8°N for the Pana Fm (Linzhou

Basin [Chen *et al.*, 2010; Dupont-Nivet *et al.*, 2010; Tan *et al.*, 2010]). The red line in Figure 9 denotes the average of these four formations (~12°N). Looking closely at the new data from the Pana Formation, a high discrepancy in paleolatitudes from this formation becomes evident (short green lines in Figure 9) diverging largely from 5.2°N [Chen *et al.*, 2010] to 32.7°N [Tan *et al.*, 2010].

[34] The work of Achache *et al.* [1984] and Westphal *et al.* [1983] already yielded similar paleolatitudes of ~13°N and ~8°N, respectively, however, the Achache *et al.* data were put into question because of a possible secondary overprint and the significance of the Westphal *et al.* results is limited because only two sites were sampled. Data from the intrusives, ophiolites and flysch in the suture zone are also available, but it is not clear whether these rocks were magnetized at the position where the continents collided. Nevertheless, it is worth noting that the inclinations from these units give paleolatitudes of 7–10°N [Klootwijk *et al.*, 1979], 10–20°N [Pozzi *et al.*, 1984] and 3°S–8°N [Abrajevitch *et al.*, 2005]. We also do not consider results from the granites directly adjacent to the IYSZ as this zone is strongly affected by large vertical-axis rotations and also inclinations scatter considerably [Otofujii *et al.*, 1989]. For the Cretaceous there are several data which can be considered as meaningful. Most of them stem from the mid-Cretaceous sedimentary Shexing Formation (mostly red beds) indicating paleolatitudes (for the reference point) of ~7°N [Lin and Watts, 1988], ~11°N [Achache *et al.*, 1984], ~21°N [Westphal *et al.*, 1983], and ~12°N [Tan *et al.*, 2010]. Possible inclination shallowing is a critical issue for the validity of data from sedimentary rocks. Tan *et al.* [2010] correct their data by the E/I analysis [Tauxe and Kent, 2004] and calculate a corrected paleolatitude of ~22°N, however, although the test can be useful to identify the existence of inclination shallowing one should be careful with interpreting corrected results quantitatively. Further Cretaceous data are available from the Nagqu and Qelico volcanics yielding paleolatitudes of ~17°N and ~18°N, respectively [Lin and Watts, 1988], and from volcanics intercalated with sediments [Tan *et al.*, 2010] which give a somewhat more northerly position at ~23°N. The Cretaceous and Cenozoic paleolatitudes coincide relatively well and suggest that the southern margin of Eurasia (Lhasa Block) was at an approximately constant latitude from Upper Cretaceous until the onset of the collision with India. A further statistically sound result from Cretaceous limestones in the far west of the Lhasa Block [Chen *et al.*, 1993] gives a similar paleolatitude of ~11°N (corresponding to ~8°N for the reference point) indicating that the southern Eurasian margin was quite linear prior to collision. We are therefore confident that the paleogeographic position shown in Figure 9 (red bold line and shaded area) is a good estimate for the precollisional southern margin of the Lhasa Block. It implies ~1950 km north-south shortening within the Tibetan Plateau by intra-continental deformation.

[35] The position of the northern margin of India around the time of the collision in Figure 9 is determined by the results of Patzelt *et al.* [1996] for the 58.5 Ma Zongpu Formation at Gamba and Duela (Table 1). A large extent of “Greater India” can be concluded from these data. The northward drift from 58.5 to 45 Ma follows the apparent polar wander path (APWP) of Besse and Courtillot [2002, 2003]. Another 14 sites from the Maastrichtian Zongshan Formation

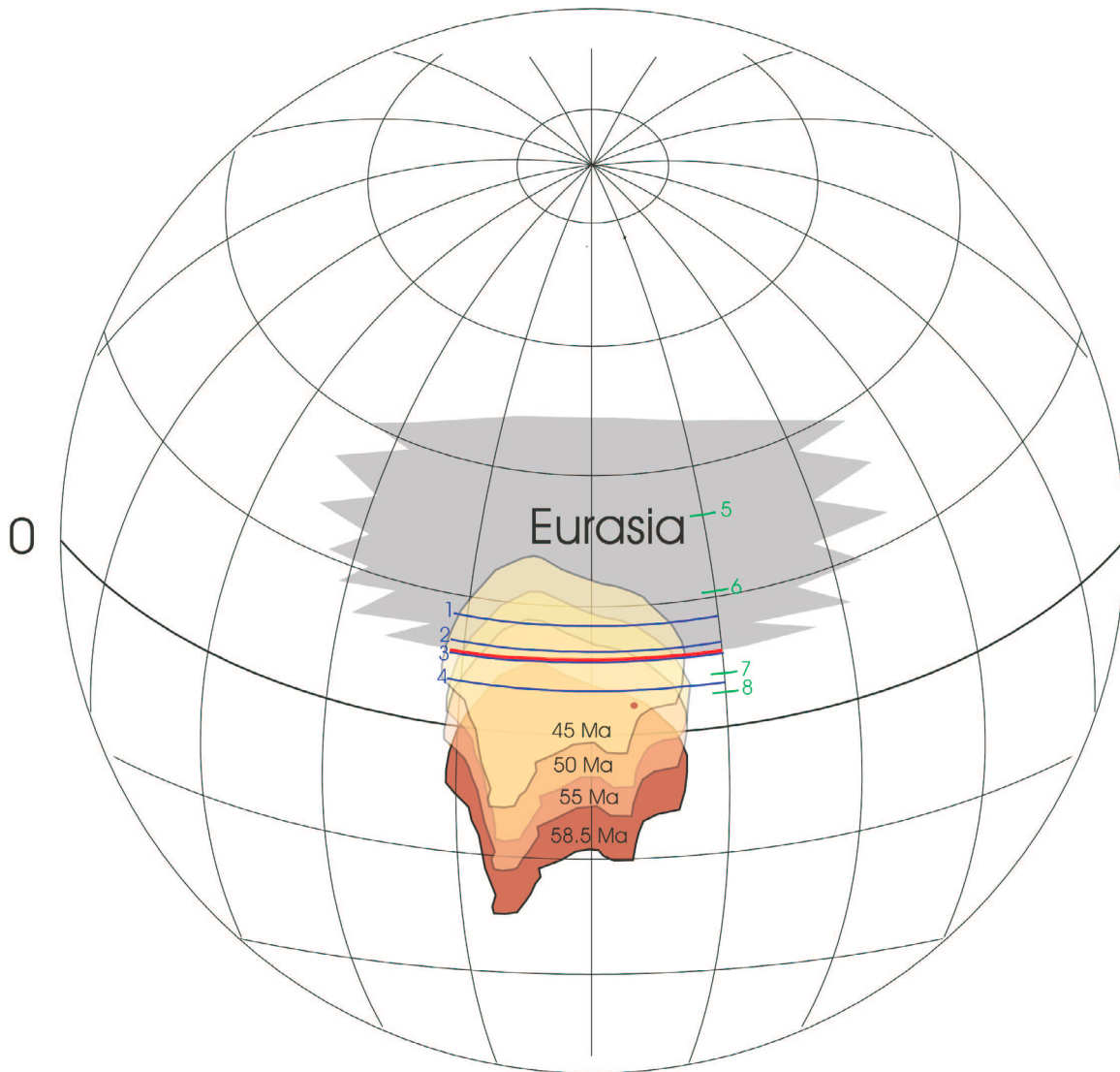


Figure 9. Paleogeographic reconstruction of the position of India during 58.5 to 45 Ma and the southern margin of Eurasia around 50 Ma (shaded area). The dot at the northern margin of “Greater India” corresponds to the paleolatitude of *Patzelt et al.* [1996] that is determined for the Zongpu group with an age of 58.5 Ma. The drift rate of India is according to the apparent polar wander path of *Besse and Courtillot* [2002]. New paleomagnetic results from four different units of the Linzizong Formation are considered for the determination of the precollisional or syncollisional southern margin of Eurasia (blue lines): 1, Pana Formation (Fm) (mean value of data from *Dupont-Nivet et al.* [2010], *Tan et al.* [2010], and *Chen et al.* [2010]); 2, dykes intruded in the Nianbo Fm [*Liebke et al.*, 2010]; 3, Nianbo Fm (mean value of data from *Chen et al.* [2010] and *Sun et al.* [2010]); 4, Dianzhong Fm [*Chen et al.*, 2010]. The red line displays the mean value of all four formations. Green lines show the different results from the Pana Fm (5, *Tan et al.* [2010]; 6, *Dupont-Nivet et al.* [2010]; 7, *Chen et al.* [2010] for the Linzhou Basin; 8, *Chen et al.* [2010] for the Namling Basin). All paleomagnetic data are listed in Table 1. Latitude lines are in 20° increments up to 80°N.

studied by *Patzelt et al.* [1996] confirm the results from the Zongpu Formation. *Besse et al.* [1984] derived a much smaller extent of “Greater India” from the Zhepure Shan Formation at Tingri, however based on five sites only. Recently published data for the Zongpu Formation at Tingri [*Tong et al.*, 2008] reside on three sites only and were determined by great circle intersections; they have to be considered as very preliminary at this stage. Some available

data from older Cretaceous rock units [*Appel et al.*, 1998; *Klootwijk and Bingham*, 1980] are based on only one or two sampling sites and pre-Cretaceous data are unsuitable to determine the extent of the northern margin due to strong counterclockwise rotation of India.

[36] In summary, Figure 9 and the data presented above demonstrate that both continental margins achieved their initial contact in early Eocene. *Liebke et al.* [2010] determine

Table 1. Summary of Paleomagnetic Results Discussed in This Paper^a

Lithology	Site Location		Age	N _{si}	D _g	I _g	D _s	I _s	α ₉₅	Paleolat	VGP		Ref ^b
	Locality	(°N/°E)									Lat	Long	
<i>Tertiary Data (Linziyong Volcanic Rocks)</i>													
LVR	Linzhou	(29.9/91.0)	IEc	8	170.1	-33.0	170.9	-25.5	11.0	12.7	71.5	300.0	1
LVR	Linzhou	(29.9/91.0)	IEc	2	4.0	31.0	0.0	18.0	30.6	8.3	69.3	271.0	2
Pana Fm (volc.)	Linzhou	(30.5/91.1)	IEc	24	20.8	71.7	13.5	40.0	5.6	21.1#	75.7	210.6	3
Pana Fm (volc.)	Linzhou	(29.9/91.2)	IEc	9	339.0	80.0	0.0	53.0	5.0	32.7#	86.3	91.2	4
Pana Fm (volc.)	Linzhou	(30.0/91.1)	IEc	5	3.7	40.6	3.3	12.3	12.9	5.2#	66.0	263.0	5
Pana Fm (volc.)	Namling	(29.8/89.2)	IEc	5	348.1	43.5	353.6	17.5	37.7	8.1#	68.3	286.5	5
Pana Fm (sed.)	Namling	(29.8/89.2)	IEc	4	348.9	41.8	345.5	16.9	16.8	7.7	64.9	304.8	5
Mean Pana Fm (Without Sediments)				4	358.2	59.1	358.1	27.8		16.8*			
Dykes (in Nianbo Fm)	Linzhou	(30.0/91.1)	IEc	10	13.5	40.9	15.4	27.2	9.7	13.2*	68.9	225.4	6
Nianbo Fm (volc.)	Linzhou	(29.9/91.2)	uPc	5	2.4	49.0	353.7	21.9	16.5	10.6	70.6	290.1	5
Nianbo Fm (sed.)	Linzhou	(29.9/91.2)	uPc	4	12.8	67.4	359.9	16.3	20.7	7.4	68.4	271.5	5
Nianbo Fm (volc.)	Mendui	(30.1/90.9)	uPc	14	350.1	46.9	359.0	26.1	9.2	12.6	73.6	274.3	7
Mean Nianbo Fm (Without Sediments)				2	355.8	47.7	355.9	23.5		11.6*			
Dianzhong Fm (volc.)	Namling	(29.8/89.2)	IPc	7	154.2	-30.4	159.6	-9.0	8.8	3.5	58.2	310.5	5
Dianzhong Fm (volc.)	Linzhou	(29.9/91.2)	IPc	8	193.9	-40.2	185.5	-21.1	8.5	9.9	70.3	255.0	5
Mean Dianzhong Fm					172.3	-36.6	171.6	-15.4		6.7*			
<i>Cretaceous Data</i>													
Shexing Fm (sed.)	Linzhou	(29.9/91.2)	uCr	43	346.0	48.0	350.2	23.5	2.5	11.6	70.2	300.5	4
Intercalated volc.	Linzhou	(29.9/91.2)	uCr	21	335.9	-13.9	202.6	-41.9	4.4	22.9	69.1	191.7	4
Sandst, limestone	Domar	(33.8/80.4)	Cr	14	13.3	20.7	6.2	22.1	5.5	7.9	67.0	244.7	8
Shexing Fm (sed.)	Linzhou (N)	(32.0/91.5)	uCr	6	335.9	41.9	338.7	25.4	8.9	11.0	63.0	322.7	1
Shexing Fm (sed.)	Linzhou (S)	(29.9/91.0)	uCr	8	1.4	25.1	354.3	22.6	8.3	11.0	71.1	288.7	1
Shexing Fm (sed.)	Linzhou	(29.9/91.2)	uCr	8	8.0	59.0	357.0	15.0	6.7	6.8	67.6	279.0	9
Shexing Fm (sed.)	Linzhou	(29.9/91.0)	uCr	6	346.0	18.0	333.0	38.0	8.0	20.9	64.3	347.9	2
Qelico (volc.)		(31.7/91.0)	uCr	4	333.0	44.0	347.0	36.0	16.5	17.6	73.5	318.9	9
Nagqu (volc.)		(31.5/92.0)	uCr	9	322.0	54.0	358.0	35.0	6.0	16.9	77.7	280.9	9
Zongpu Fm	Gamba/Gulu	(28.2/88.9)	Pc	14	171.9	-20.6	176.2	-7.9	7.5	4.7	65.5	278.1	10

^aLVR, Linziyong volcanic rocks (undifferentiated); Fm, formation; volc., volcanics; sed., sediments; sandst, sandstone. Age: l, lower; u, upper; Ec, Eocene; Pc, Paleocene; Cr, Cretaceous; N_{si}, number of sites; D_g, declination (geographic coordinate); I_g, inclination (geographic coordinate); D_s, declination (stratigraphic coordinate); I_s, inclination (stratigraphic coordinate); α₉₅, 95% confidence limit (for stratigraphic data); Paleolat, paleolatitude for a reference point at 29°N/90°E on the suture zone; VGP, virtual geomagnetic pole; lat, latitude; long, longitude; Ref, reference; *, paleolatitudes drawn in blue in Figure 9 (values are bolded in Table 1), #, paleolatitudes drawn in green in Figure 9 (values are bolded in Table 1). Listed data from sediments are not corrected for possible inclination shallowing.

^bRefs: 1, *Achache et al.* [1984]; 2, *Westphal et al.* [1983]; 3, *Dupont-Nivet et al.* [2010]; 4, *Tan et al.* [2010]; 5, *Chen et al.* [2010]; 6, *Liebke et al.* [2010]; 7, *Sun et al.* [2010]; 8, *Chen et al.* [1993]; 9, *Lin and Watts* [1988]; 10, *Patzelt et al.* [1996].

the age of collision at 53–49 Ma at 90°E; *Dupont-Nivet et al.* [2010] derive a slightly younger age of 48 Ma (57–40 Ma within 95% confidence limits) and *Chen et al.* [2010] calculate a collisional time of 65–50 Ma (or narrowed down to 60–55 Ma assuming a 950 km extent of Greater India). These results are all in agreement with the generally considered age of the India-Asia collision determined using a variety of approaches, as outlined in section 1. The paleomagnetic results from the Pana Formation [*Tan et al.*, 2010] give a younger collision age of 43 Ma. The data in their study are carefully analyzed and valuable. However, caution should be taken when considering whether the sampled volcanic tuffs could represent a short-term large eruption event potentially leading to a snapshot record of the Earth magnetic field at high inclination. A still younger age for India-Asia collision is proposed with the paleomagnetic study of *Aitchison et al.* [2007] who calculate that there was considerable separation between the two continents at 55 Ma and thus they consider collision at this time highly unlikely. *Aitchison et al.* use the APWP plus a reasonable “Greater India” extent for the determination of India’s northern margin at 55 Ma. *Ali and Aitchison* [2005] have compiled a large number of different

models for “Greater India”. The model for the extent of India and the northward movement used by *Aitchison et al.* [2007] is similar to that derived in Figure 9 based on *Patzelt et al.* [1996]. For the Asian side, *Aitchison et al.* ignore any post-collisional north-south shortening within the Tibetan Plateau and place the southern margin of the Lhasa Block at around 30°N by simply using the APWP of Eurasia. We consider this an unjustified approach. To relocate the southern margin of the Lhasa Block prior to collision one requires data from the Lhasa Block itself, as outlined above. *Aitchison et al.* considered that no reliable Cenozoic data from this region were available at the time of writing. We consider: first, that new results subsequently published by *Liebke et al.* [2010], *Dupont-Nivet et al.* [2010], *Chen et al.* [2010], *Sun et al.* [2010], and *Tan et al.* [2010] improve the database for the Paleogene considerably. Second, according to Eurasia’s rather stable APWP since the Cretaceous and the fact that the Lhasa Block was accreted to Eurasia in Early Cretaceous [*Baxter et al.*, 2009] crustal deformation and paleogeographical changes in this region were probably very minor since the beginning of Cretaceous until the time of the India-Asia collision.

5.2. Timing of Cessation of Marine Facies

[37] The age of the youngest marine facies in the Qumiba section, dated by Wang *et al.* [2002] at ~34 Ma, is by far the youngest marine facies reported in the suture zone so far, and is used by Aitchison *et al.* [2007] as supporting evidence for a later timing of India-Asia collision. However, as summarized in section 2, this age is disputed by Zhu *et al.* [2005]. While Wang *et al.* consider the entire succession to be entirely marine with the Enba Member to be of NP15–17 age, and the disconformably overlying Zhaguo Member to be of NP18–20 age, Zhu *et al.* consider the Enba Formation to be marine facies of P8 age (50.6 Ma), and the disconformably overlying Zaguo Formation to be considerably younger continental facies, containing reworked fauna. However, it must be recognized that the fauna recorded by Wang *et al.*, if correctly identified, would still record the youngest evidence of marine facies in the Tethyan Himalaya, whether reworked or in situ and furthermore, if the Zhaguo Member facies interpretation of Wang *et al.* is adopted, the possibility of the prior existence of younger marine sedimentary rocks, removed by overthrusting, cannot be ruled out.

[38] Our data (section 3) show that regardless of the nature of the contact between the Enba and Zhaguo members, we find no evidence for marine organisms younger than nannofossil zones NP12 or foraminifera zones P7–8 (ca. 50.6 Ma) in this unit, reworked or in situ. We therefore conclude that there is no recorded evidence of continuation of marine facies to the end of the Eocene at this locality as previously reported, and this sedimentary section cannot be used to support the contention that India-Asia collision occurred at ~34 Ma. We also reiterate, as noted in section 1, the time of cessation of marine facies provides only a minimum age to collision since marine conditions may persist on continental crust for some time post collision.

5.3. Beginning of Continental Molasse Sedimentation in the Suture Zone and Regional Sedimentation Patterns

[39] The earliest known molasse containing detritus derived from both sides of the suture zone has recently been redated from Eocene to Miocene [Aitchison *et al.*, 2002]. However, we note that while the redating of this molasse does indeed remove this line of evidence for an Eocene collision, it does not require the collision to be Miocene; it only provides an “upper bound” to the age, as Aitchison *et al.* acknowledge [see also Davis *et al.*, 2004]. Aitchison *et al.* [2007] also note the delay between proposed 50 Ma collision and onset of significant sedimentation in the foreland basin and more distal basins offshore. The cause of the time gap between collision and significant recorded erosion from the orogen is intriguing, but a later collision is not the only way to explain these data. As Aitchison *et al.* point out, a number of explanations have been proposed for different basins e.g., lack of preservation of early material due to overthrusting, cratonward migration of a forebulge, redistribution of the load, slab breakoff, negligible erosion due to an arid climate, and early subdued topography which can be attributed to a variety of reasons [DeCelles *et al.*, 1998; Guillot *et al.*, 2003; Najman *et al.*, 2004; Najman *et al.*, 2008]. Furthermore, as pointed out by Garzanti [2008] a delay to significant sedimentation following collision is not an unusual feature, also

found, for example, in the Alpine orogen [Garzanti and Malusa, 2008].

5.4. Ending of Andean-Type Calc-Alkaline Magmatism on the Southern Margin of Asia

[40] Aitchison *et al.* [2007] consider that subduction related magmatism continued until at least 37 Ma thus providing supporting evidence for a younger age of collision. However, we believe the timing of cessation of subduction related magmatism is difficult to define. Identification of the youngest subduction-related magmatism is not straightforward, since calc-alkaline magmatism, typical of subduction-related settings, may persist into collisional regimes [Harris *et al.*, 1990]. Ages as young as late Eocene have been recognized in the Trans-Himalayan batholith, and discussed in the context of their implications for determining the closure of Tethys for over two decades [Searle *et al.*, 1987] and then, as now, these implications are not clear. Miller *et al.* [1999] and Harrison *et al.* [2000] record ages of 16–17 Ma and 30 Ma for calc-alkaline igneous rocks in southern Tibet which they consider have geochemical signatures that are similar to undoubted subduction-related suites such as the Trans-Himalaya. Since the younger age range is clearly postcollisional, Harrison *et al.* consider that calc-alkaline magmatism is thus a poor indicator of the timing of active subduction of oceanic lithosphere beneath a continental margin, and provide other potential explanations for its occurrence. By contrast, Chung *et al.* [2003, 2005] disagree that the geochemistry is similar to the subduction-related Trans-Himalaya and reinterpret the rocks as collision-related adakites. In their view, “soft collision” (first contact between the continental margins) occurred around 60 Ma. Slab roll back accompanied by southward migration of asthenospheric convection beneath Tibet was responsible for the Cenozoic magmatism, which was terminated by slab breakoff at ~45 Ma which resulted in cessation of subduction and “hard collision.”

[41] Therefore the interpretation of the tectonic environment of these rocks is not clear-cut. What is clear is that calc-alkaline magmatism with adakite-like characteristics in southern Tibet is now known to range in age from Early Cretaceous to the late Miocene, and so has formed throughout periods of subduction of oceanic lithosphere, continent collision and postcollision tectonics. Since these magmas have formed in highly diverse tectonic settings, their only shared petrogenetic factor is the presence of garnet in the source which reduces the HREE and Y abundances in the melt, irrespective of tectonic setting [Zhang *et al.*, 2010]. Thus the geochemistry of these rocks cannot unequivocally be used to date the timing of cessation of subduction and subsequent continent collision.

5.5. Initiation of Major Thrusting

[42] Aitchison *et al.* [2007] contend that initiation of major collision-related thrust systems is an immediate response to all active collisions on earth today. With regard to the timing of development of collision-related thrust systems in the Himalaya, Aitchison *et al.* in fact acknowledge that “Paleocene-early Eocene regional crustal shortening . . . is recorded in the Tethyan Himalaya” which, we note, would be entirely consistent with a rapid response to India-Asia collision around 55–50 Ma. However, Aitchison *et al.* prefer to

interpret this tectonism to be the result of collision at 55 Ma between an intraoceanic arc (Dazuqu, Bainang and Zedong terrains of south Tibet) [Aitchison *et al.*, 2000] and India, prior to India-Asia collision.

6. Conclusions

[43] The Tethyan Himalayan Qumiba section in southern Tibet records the transition from the ca 53–54 Ma aged carbonates of the Zephure Shan Formation to the 50.6–52.8 Ma aged clastics of the overlying Pengqu Formation. Our biostratigraphic dating of the Pengqu Formation at 50.6–52.8 Ma is consistent with the dating of Zhu *et al.* [2005] at this locality, but at variance with the middle to late Eocene age of Wang *et al.* [2002]. In our view, these rocks do not therefore provide evidence of a latest Eocene (late Priabonian) cessation to the time of marine facies in the orogen as previously proposed and cannot be used to support the proposal of India-Asia collision <35 Ma [Aitchison *et al.*, 2007].

[44] Cretaceous–earliest Eocene U–Pb ages of detrital zircons from the Pengqu Formation are consistent with derivation from the Asian Trans-Himalaya and inconsistent with derivation from the Indian plate, and thus we interpret the Pengqu Formation to represent the record of the first arrival of Asian detritus on to the Indian plate at this locality, thereby constraining India-Asia collision at prior to 50.6 Ma. Provenance from a Late Jurassic intraoceanic arc colliding with India at this time has also been proposed for these rocks [Aitchison *et al.*, 2007], with India-Asia collision occurring only in the Oligocene, but until zircons of similar age to the Pengqu Formation are recorded in this arc, and zircons of Jurassic age are found in the Pengqu Formation, we prefer to interpret the detritus as Asian derived.

[45] Additional evidence for a proposed Oligocene India-Asia collision has been put forward by Aitchison *et al.* [2007], namely (1) their reconstruction of the relative positions of India and Asia in the Cenozoic show wide separation of the continents at 55 Ma and (2) their geological evidence of the time of cessation of marine facies (as discussed above), the age of the oldest recorded postcollisional molasse and onset of major orogen-derived sedimentation, the timing of cessation of subduction-related magmatism, and the timing of major thrusting in the orogen, are all proposed to have occurred later than previously believed. We provide alternative arguments for each of these lines of evidence. We provide a synthesis of palaeomagnetic data from which we interpret that initial contact between the continents occurred in the early Eocene. We argue that a delay to the timing of onset of erosion from the orogen may be explained by later collision, but could equally well be explained by a number of other factors. We argue that the calc-alkaline rocks formed in highly diverse tectonic settings not restricted to subduction regimes. Finally we reiterate the fact that major thrusting is recorded in the orogen shortly after collision.

[46] We therefore consider that the view of Aitchison *et al.* [2007], that the geological record and relative positions of India and Asia “demand” that the continental collision occurred no earlier than the Oligocene, is overstated. Collision of India with an intraoceanic arc at ~55 Ma may well be a viable theory worthy of further investigation, and certainly collisions between island arcs and continents are capable of producing significant orogeny, e.g., the Taconic Orogeny,

USA [Stanley and Ratcliffe, 1985]. However, available evidence does not currently “demand” that collision between India and Asia occurred no earlier than the Oligocene; available evidence also remains consistent with collision by ~50 Ma.

[47] **Acknowledgments.** We thank Kyle Larson (Queen’s University at Kingston, Canada) for field assistance, Angus Calder (University of St Andrews, UK) for carrying out the illite crystallinity analyses, and Chen Hehai (CAS, Beijing, China) for the mineral separations. Nigel Harris is acknowledged for his expertise and input to the magmatic discussion in this paper and S.-L. Chung and G. Gehrels are acknowledged for providing access to their databases of compiled U–Pb data for the Trans-Himalaya and Tethyan Himalaya, respectively. Tseyang and Tashi are thanked for guiding, cooking, and driving during fieldwork. This work was funded by grants to Najman from the Royal Society and NERC (grant NE/D000092/1). Reviews by Jonathan Aitchison, Mary Leech, and two anonymous reviewers are acknowledged.

References

- Abrajavitch, A. V., *et al.* (2005), Neotethys and the India-Asia collision: Insights from a palaeomagnetic study of the Dazuqu ophiolite, southern Tibet, *Earth Planet. Sci. Lett.*, **233**, 87–102, doi:10.1016/j.epsl.2005.02.003.
- Achache, J., V. Courtillot, and Z. Y. Xiu (1984), Palaeogeographic and tectonic evolution of southern Tibet since middle Cretaceous time: New palaeomagnetic data and synthesis, *J. Geophys. Res.*, **89**, 10,311–10,339.
- Aikman, A. B., *et al.* (2008), Evidence for early (>44 Ma) Himalayan crustal thickening, Tethyan Himalaya, southeastern Tibet, *Earth Planet. Sci. Lett.*, **274**, 14–23, doi:10.1016/j.epsl.2008.06.038.
- Aitchison, J. C., *et al.* (2000), Remnants of a Cretaceous intra-oceanic subduction system within the Yarlung-Zangbo suture (southern Tibet), *Earth Planet. Sci. Lett.*, **183**, 231–244, doi:10.1016/S0012-821X(00)00287-9.
- Aitchison, J. C., *et al.* (2002), New constraints on the India-Asia collision: The lower Miocene Gangrinboche conglomerates, Yarlung Tsangpo suture zone, SE Tibet, *J. Asian Earth Sci.*, **21**, 251–263, doi:10.1016/S1367-9120(02)00037-8.
- Aitchison, J. C., *et al.* (2003), Stratigraphic and sedimentological constraints on the age and tectonic evolution of the Neotethyan ophiolites along the Yarlung Tsangpo suture zone, in *Ophiolites in Earth History*, edited by Y. Dilek and R. T. Robinson, *Geol. Soc. Spec. Publ.*, vol. 218, 147–164.
- Aitchison, J. C., J. R. Ali, and A. M. Davis (2007), When and where did India and Asia collide?, *J. Geophys. Res.*, **112**, B05423, doi:10.1029/2006JB004706.
- Ali, J. R., and J. C. Aitchison (2005), Greater India, *Earth Sci. Rev.*, **72**, 169–188, doi:10.1016/j.earscirev.2005.07.005.
- Appel, E., *et al.* (1998), Palaeomagnetic results from the Late Cretaceous and early Tertiary limestones from Tingri area, southern Tibet, China, *J. Nepal Geol. Soc.*, **18**, 113–124.
- Baxter, A. T., *et al.* (2009), Radiolarian age constraints on Mesotethyan ocean evolution, and their implications for development of the Bangong-Nujiang suture, Tibet, *J. Geol. Soc.*, **166**, 689–694, doi:10.1144/0016-76492008-128.
- Besse, J., and V. Courtillot (2002), Apparent and true polar wander and the geometry of the geomagnetic field over the last 200 Myr, *J. Geophys. Res.*, **107**(B11), 2300, doi:10.1029/2000JB000050.
- Besse, J., and V. Courtillot (2003), Correction to “Apparent and true polar wander and the geometry of the geomagnetic field over the last 200 Myr”, *J. Geophys. Res.*, **108**(B10), 2469, doi:10.1029/2003JB002684.
- Besse, J., *et al.* (1984), Paleomagnetic estimates of crustal shortening in the Himalayan thrusts and Zangbo suture, *Nature*, **311**, 621–626, doi:10.1038/311621a0.
- Blenkinsop, T. G. (1988), Definition of low-grade metamorphic zones using illite crystallinity, *J. Metamorph. Geol.*, **6**, 623–628, doi:10.1111/j.1525-1314.1988.tb00444.x.
- Blondeau, A., *et al.* (1986), Disparition des formations marines a l’eoecene inferieur en Himalaya, *Sci. Terre: Mem.*, **47**, 103–111.
- Booth, A. L., *et al.* (2004), U–Pb zircon constraints on the tectonic evolution of southeastern Tibet, Namche Barwa area, *Am. J. Sci.*, **304**, 889–929, doi:10.2475/ajs.304.10.889.
- Bown, P. R., and J. R. Young (1998), Techniques, in *Calcareous Nannofossil Biostratigraphy*, edited by P. R. Bown, pp. 16–28, Kluwer Acad., London.

- Bralower, T. J., and J. Mutterlose (1995), Calcareous nannofossil biostratigraphy of ODP Site 865, Allison Guyot, Central Pacific Ocean: A tropical Paleogene reference section, *Proc. Ocean Drill. Program Sci. Results*, *143*, 31–74.
- Chen, J. S., et al. (2010), New constraints on the onset of the India-Asia collision: Paleomagnetic reconnaissance on the Linzizong Group in the Lhasa Block, China, *Tectonophysics*, *489*, 189–209, doi:10.1016/j.tecto.2010.04.024.
- Chen, Y., J.-P. Cogné, V. Courtillot, P. Tapponnier, and X. Y. Zhu (1993), Cretaceous paleomagnetic results from western Tibet and tectonic implications, *J. Geophys. Res.*, *98*, 17,981–17,999.
- Chu, M.-F., et al. (2006), Zircon U-Pb and Hf isotope constraints on the Mesozoic tectonics and crustal evolution of southern Tibet, *Geology*, *34*, 745–748, doi:10.1130/G22725.1.
- Chung, S.-L., et al. (2003), Adakites from continental collision zones: Melting of thickened lower crust beneath southern Tibet, *Geology*, *31*, 1021–1024, doi:10.1130/G19796.1.
- Chung, S.-L., et al. (2005), Tibetan tectonic evolution inferred from spatial and temporal variations in post-collisional magmatism, *Earth Sci. Rev.*, *68*, 173–196, doi:10.1016/j.earscirev.2004.05.001.
- Crittelli, S., and E. Garzanti (1994), Provenance of the lower Tertiary Murree Redbeds (Hazara-Kashmir Syntaxis, Pakistan) and initial rising of the Himalayas, *Sediment. Geol.*, *89*, 265–284, doi:10.1016/0037-0738(94)90097-3.
- Davis, A. M., et al. (2004), Conglomerates record the tectonic evolution of the Yarlung-Tsangpo suture zone in southern Tibet, in *Aspects of the Tectonic Evolution of China*, edited by J. Malpas et al., *Geol. Soc. Spec. Publ.*, vol. 226, 235–246.
- DeCelles, P. G., G. Gehrels, J. Quade, and T. Ojha (1998), Eocene-early Miocene foreland basin development and the history of Himalayan thrusting, western and central Nepal, *Tectonics*, *17*, 741–765, doi:10.1029/98TC02598.
- de Sigoyer, J., et al. (2000), Dating the Indian continental subduction and collisional thickening in the northwest Himalaya: Multichronology of the Tso Moriri eclogites, *Geology*, *28*, 487–490, doi:10.1130/0091-7613(2000)28<487:DTICSA>2.0.CO;2.
- Dickinson, W. R. (1985), Interpreting provenance relations from detrital modes of sandstones, in *Provenance of Arenites*, edited by G. G. Zuffa, pp. 333–361, Reidel, Dordrecht, Netherlands.
- Ding, L., P. Kapp, and X. Wan (2005), Paleocene-Eocene record of ophiolite obduction and initial India-Asia collision, south central Tibet, *Tectonics*, *24*, TC3001, doi:10.1029/2004TC001729.
- Dupont-Nivet, G., et al. (2010), Paleolatitude and age of the Indo-Asia collision: Paleomagnetic constraints, *Geophys. J. Int.*, *182*, 1189–1198, doi:10.1111/j.1365-246X.2010.04697.x.
- Fuchs, G., and H. Willems (1990), The final stages of sedimentation in the Tethyan zone of Zaskar and their geodynamic significance (Ladakh-Himalaya), *Jahrb. Geol. Bundesanstalt*, *133*, 259–273.
- Galbraith, R. F., and P. F. Green (1990), Estimating the component ages in a finite mixture, *Radiat. Meas.*, *17*, 197–206, doi:10.1016/1359-0189(90)90035-V.
- Garzanti, E. (2008), Comment on “When and where did India and Asia collide?” by Jonathan C. Aitchison, Jason, R. Ali, and Aileen M. Davis, *J. Geophys. Res.*, *113*, B04411, doi:10.1029/2007JB005276.
- Garzanti, E., and M. G. Malusa (2008), The Oligocene Alps: Domal unroofing and drainage development during early orogenic growth, *Earth Planet. Sci. Lett.*, *268*, 487–500, doi:10.1016/j.epsl.2008.01.039.
- Garzanti, E., and G. Vezzoli (2003), A classification of metamorphic grade in sands based on their composition and grade, *J. Sediment. Res.*, *73*, 830–837, doi:10.1306/012203730830.
- Garzanti, E., et al. (1987), Sedimentary Record of the Northward Flight of India and Its Collision with Eurasia (Ladakh Himalaya, India), *Geodin. Acta*, *1*, 297–312.
- Garzanti, E., et al. (2007), Orogenic belts and orogenic sediment provenances, *J. Geol.*, *115*, 315–334, doi:10.1086/512755.
- Gehrels, G. E., V. A. Valencia, and J. Ruiz (2008), Enhanced precision, accuracy, efficiency, and spatial resolution of U-Pb ages by laser ablation-multicollector-inductively coupled plasma-mass spectrometry, *Geochem. Geophys. Geosyst.*, *9*, Q03017, doi:10.1029/2007GC001805.
- Gradstein, F. M., and J. G. Ogg (2004), Geologic time scale 2004: Why, how, and where next! *Lethaia*, *37*, 175–181, doi:10.1080/00241160410006483.
- Gradstein, F. M., et al. (2004), A new geologic time scale, with special reference to Precambrian and Neogene, *Episodes*, *27*, 83–100.
- Green, O. R., et al. (2008), Cretaceous-Tertiary carbonate platform evolution and the age of the India-Asia collision along the Ladakh Himalaya (Northwest India), *J. Geol.*, *116*, 331–353, doi:10.1086/588831.
- Guillot, S., E. Garzanti, D. Baratoux, D. Marquer, G. Mahéo, and J. de Sigoyer (2003), Reconstructing the total shortening history of the NW Himalaya, *Geochem. Geophys. Geosyst.*, *4*(7), 1064, doi:10.1029/2002GC000484.
- Harris, N. B. W., et al. (1990), Cretaceous plutonism in central Tibet: An example of post-collisional magmatism?, *J. Volcanol. Geotherm. Res.*, *44*, 21–32, doi:10.1016/0377-0273(90)90009-5.
- Harrison, T. M., A. Yin, M. Grove, O. Lovera, F. Ryerson, and X. Zhou (2000), The Zedong window: A record of superposed Tertiary convergence in southeastern Tibet, *J. Geophys. Res.*, *105*, 19,211–19,230.
- Henderson, A. L., Y. Najman, R. Parrish, M. Boudagher-Fadel, D. Barford, E. Garzanti, and S. Ando (2010), Geology of the Cenozoic Indus Basin sedimentary rocks: Palaeoenvironmental interpretation of sedimentation from the western Himalaya during the early phases of India-Eurasia collision, *Tectonics*, doi:10.1029/2009TC002651, in press.
- Hodges, K. V. (2000), Tectonics of the Himalaya and southern Tibet from two perspectives, *Geol. Soc. Am. Bull.*, *112*, 324–350, doi:10.1130/0016-7606(2000)112<324:TOTHAS>2.0.CO;2.
- Hu, X., et al. (2009a), Provenance of Lower Cretaceous Wölong Volcanics in the Tibetan Tethyan: Implications for the final breakup of Eastern Gondwana, *Sediment. Geol.*, *223*, 193–205, doi:10.1016/j.sedgeo.2009.11.008.
- Hu, X., J. Wang, L. Jansa, F. Wu, and J. Wu (2009b), Stratigraphic and provenance evidence for recognition of an underfilled foreland basin in central Himalaya: Implication for timing of India-Asia initial collision, *Eos Trans. AGU*, *90*(52), Fall Meet. Suppl., Abstract T31E-03.
- Ingersoll, R. V., et al. (1993), The effect of sampling scale on actualistic sandstone petrofacies, *Sedimentology*, *40*, 937–953, doi:10.1111/j.1365-3091.1993.tb01370.x.
- Jaeger, J. J., et al. (1989), Paleontological view of the ages of the Deccan Traps, the Cretaceous/Tertiary boundary, and the India-Asia collision, *Geology*, *17*, 316–319, doi:10.1130/0091-7613(1989)017<0316:PVOTAO>2.3.CO;2.
- Jain, A. K., et al. (2009), Detrital-zircon fission-track ages from the lower Cenozoic sediments, NW Himalayan foreland basin: Clues for exhumation and denudation of the Himalaya during the India-Asia collision, *Geol. Soc. Am. Bull.*, *121*, 519–535, doi:10.1130/B26304.1.
- Ji, W.-Q., et al. (2009), Zircon U-Pb geochronology and Hf isotopic constraints on petrogenesis of the Gangdese batholith, southern Tibet, *Chem. Geol.*, *262*, 229–245, doi:10.1016/j.chemgeo.2009.01.020.
- Kapp, P., et al. (2005), Cretaceous-Tertiary shortening, basin development, and volcanism in central Tibet, *Geol. Soc. Am. Bull.*, *117*, 865–878, doi:10.1130/B25595.1.
- Klootwijk, C. T., and D. K. Bingham (1980), The extent of Greater India: 3. Paleomagnetic data from the Tibetan sedimentary series, Thakola region, Nepal Himalaya, *Earth Planet. Sci. Lett.*, *51*, 381–405, doi:10.1016/0012-821X(80)90219-8.
- Klootwijk, C., et al. (1979), Extent of Greater India: 2. Paleomagnetic data from the Ladakh intrusives at Kargil, northwestern Himalayas, *Earth Planet. Sci. Lett.*, *44*, 47–64, doi:10.1016/0012-821X(79)90007-4.
- Klootwijk, C. T., et al. (1992), An early India-Asia contact: Paleomagnetic constraints from Ninetyeast Ridge, ODP Leg 121, *Geology*, *20*, 395–398, doi:10.1130/0091-7613(1992)020<0395:AEIACP>2.3.CO;2.
- Larson, K. P., L. Godin, W. J. Davis, and D. W. Davis (2010), Out-of-sequence deformation and expansion of the Himalayan orogenic wedge: Insight from the Chango culmination, south central Tibet, *Tectonics*, *29*, TC4013, doi:10.1029/2008TC002393.
- Leier, A. L., et al. (2007), Detrital zircon geochronology of carboniferous-Cretaceous strata in the Lhasa terrane, southern Tibet, *Basin Res.*, *19*, 361–378, doi:10.1111/j.1365-2117.2007.00330.x.
- Li, X. H., et al. (2006), Age of initiation of the India-Asia collision in the east-central Himalaya: A discussion, *J. Geol.*, *114*, 637–640, doi:10.1086/506165.
- Liebke, U., et al. (2010), Position of the Lhasa terrane prior to India-Asia collision derived from palaeomagnetic inclinations of 53 Ma old dykes of the Linzhou Basin: Constraints on the age of collision and post-collisional shortening within the Tibetan Plateau, *Geophys. J. Int.*, *182*, 1199–1215, doi:10.1111/j.1365-246X.2010.04698.x.
- Lin, J. L., and D. R. Watts (1988), Paleomagnetic results from the Tibetan Plateau, *Philos. Trans. R. Soc., A*, *327*, 239–262.
- Marsaglia, K. M., and R. V. Ingersoll (1992), Compositional trends in arc-related deep marine sand and sandstone: A reassessment of magmatic-arc provenance, *Geol. Soc. Am. Bull.*, *104*, 1637–1649, doi:10.1130/0016-7606(1992)104<1637:CTIARD>2.3.CO;2.
- McDermid, I. R. C., et al. (2002), The Zedong terrane: A Late Jurassic intra-oceanic magmatic arc within the Yarlung-Tsangpo suture zone, southeastern Tibet, *Chem. Geol.*, *187*, 267–277, doi:10.1016/S0009-2541(02)00040-2.
- Miller, C., et al. (1999), Post-collisional potassic and ultrapotassic magmatism in SW Tibet: Geochemical and Sr-Nd-Pb-O isotopic constraints for

- mantle source characteristics and petrogenesis, *J. Petrol.*, *40*, 1399–1424, doi:10.1093/petrology/40.9.1399.
- Mo, X. X., et al. (2005), Spatial and temporal distribution and characteristics of granitoids in the Gangdese, Tibet and implication of crustal growth and evolution, *Geol. J. Chin. Univ.*, *11*, 281–290.
- Najman, Y., et al. (2004), Evolution of the Himalayan foreland basin, NW India, *Basin Res.*, *16*, 1–24, doi:10.1111/j.1365-2117.2004.00223.x.
- Najman, Y., et al. (2005), Provenance of early foreland basin sediments, Nepal: Constraints to the timing and diachroneity of early Himalayan orogenesis, *Geology*, *33*, 309–312, doi:10.1130/G21161.1.
- Najman, Y., et al. (2008), The Paleogene record of Himalayan erosion: Bengal Basin, Bangladesh, *Earth Planet. Sci. Lett.*, *273*, 1–14, doi:10.1016/j.epsl.2008.04.028.
- Najman, Y., et al. (2010), The sedimentary record of India-Asia collision: An evaluation of new and existing constraints, paper presented at EGU General Assembly, Eur. Geosci. Union, Vienna, Austria.
- Nicora, et al. (1987), Evolution of the Tethys Himalaya continental shelf during Maastrichtian to Paleocene (Zanskar, India), *Riv. Ital. Paleontol. Strat.*, *92*, 439–496.
- Otofujii, Y., et al. (1989), Paleomagnetic study of western Tibet: Deformation of a narrow zone along the Indus Zangbo suture between India and Asia, *Earth Planet. Sci. Lett.*, *92*, 307–316, doi:10.1016/0012-821X(89)90055-1.
- Patzelt, A., et al. (1996), Palaeomagnetism of Cretaceous to Tertiary sediments from southern Tibet: Evidence for the extent of the northern margin of India prior to the collision with Eurasia, *Tectonophysics*, *259*, 259–284, doi:10.1016/0040-1951(95)00181-6.
- Perch-Nielson, K. (1985), Cenozoic calcareous nannofossils, in *Plankton Stratigraphy*, edited by H. M. Bolli et al., pp. 427–554, Cambridge Univ. Press, Cambridge, UK.
- Pozzi, J. P., et al. (1984), Paleomagnetism of the Xigaze ophiolite and flysch (Yarlung Zangbo suture zone, southern Tibet): Latitude and direction of spreading, *Earth Planet. Sci. Lett.*, *70*, 383–394, doi:10.1016/0012-821X(84)90022-0.
- Quidelleur, X., M. Grove, O. M. Lovera, T. M. Harrison, A. Yin, and F. J. Ryerson (1997), Thermal evolution and slip history of the Renbu Zedong Thrust, southeastern Tibet, *J. Geophys. Res.*, *102*, 2659–2679.
- Raymo, M. E., and W. F. Ruddiman (1988), Influence of late Cenozoic mountain building on ocean geochemical cycles, *Geology*, *16*, 649–653, doi:10.1130/0091-7613(1988)016<0649:IOLCMB>2.3.CO;2.
- Richter, F. M., et al. (1992), Sr isotope evolution of Seawater: The role of Tectonics, *Earth Planet. Sci. Lett.*, *109*, 11–23, doi:10.1016/0012-821X(92)90070-C.
- Scharer, U., et al. (1984), U-Pb geochronology of Gangdese (Transhimalaya) plutonism in the Lhasa-Xigaze region, Tibet, *Earth Planet. Sci. Lett.*, *69*, 311–320, doi:10.1016/0012-821X(84)90190-0.
- Searle, M. P., et al. (1987), The closing of Tethys and the tectonics of the Himalaya, *Geol. Soc. Am. Bull.*, *98*, 678–701, doi:10.1130/0016-7606(1987)98<678:TCOTAT>2.0.CO;2.
- Searle, M., et al. (1988), Collision tectonics of the Ladakh-Zanskar Himalaya [and discussion], *Philos. Trans. R. Soc., A*, *326*, 117–150.
- Stanley, R. S., and N. M. Ratcliffe (1985), Tectonic synthesis of the Taconian orogeny in western New England, *Geol. Soc. Am. Bull.*, *96*, 1227–1250, doi:10.1130/0016-7606(1985)96<1227:TSOTTO>2.0.CO;2.
- Sun, Z., et al. (2010), New paleomagnetic results of Paleocene volcanic rocks from the Lhasa Block: Tectonic implications for the collision of India and Asia, *Tectonophysics*, doi:10.1016/j.tecto.2010.05.011.
- Tagami, T., et al. (1998), Revised annealing kinetics of fission tracks in zircon and geological implications, in *Advances in Fission-Track Geochronology*, edited by P. Van den haute and F. De Corte, pp. 99–112, Kluwer Acad., Norwell, Mass.
- Tan, X. D., et al. (2010), New paleomagnetic results from the Lhasa Block: Revised estimation of latitudinal shortening across Tibet and implications for dating the India-Asia collision, *Earth Planet. Sci. Lett.*, doi:10.1016/j.epsl.2010.03.013.
- Tauxe, L., and D. V. Kent (2004), A simplified statistical model for the geomagnetic field and the detection of shallow bias in paleomagnetic inclinations: Was the ancient magnetic field dipolar?, in *Timescales of the Internal Geomagnetic Field*, *Geophys. Monogr. Ser.*, vol. 145, edited by J. E. T. Channell et al., pp. 101–115, AGU, Washington, D. C.
- Tong, Y., et al. (2008), Early Paleocene paleomagnetic results from southern Tibet, and tectonic implications, *Int. Geol. Rev.*, *50*, 546–562, doi:10.2747/0020-6814.50.6.546.
- Wang, C. S., et al. (2002), Latest marine horizon north of Qomolangma (Mt Everest): Implications for closure of Tethys seaway and collision tectonics, *Terra Nova*, *14*, 114–120, doi:10.1046/j.1365-3121.2002.00399.x.
- Weber, K. (1972), Notes on the determination of illite crystallinity, *Neues Jahrb. Mineral. Monatsh.*, *6*, 267–276.
- Weltje, G. J. (1997), End-member modelling of compositional data: Numerical-statistical algorithms for solving the explicit mixing problem, *J. Int. Assoc. Math. Geol.*, *29*, 503–549, doi:10.1007/BF02775085.
- Wen, D. R., et al. (2008), Zircon SHRIMP U-Pb ages of the Gangdese batholith and implications for Neotethyan subduction in southern Tibet, *Chem. Geol.*, *252*, 191–201, doi:10.1016/j.chemgeo.2008.03.003.
- Westphal, M., et al. (1983), Paleomagnetic data about southern Tibet (Xigang): 1. The Cretaceous formation of the Lhasa Block, *Geophys. J. R. Astron. Soc.*, *73*, 507–521.
- Willems, H., and B. Zhang (1993a), Cretaceous and lower Tertiary sediments of the Tethys Himalaya in the area of Gamba (south Tibet), Rep. 38, Berichte, Fachbereich Geowissenschaften, Univ. Bremen, Bremen, Germany.
- Willems, H., and B. Zhang (1993b), Cretaceous and lower Tertiary sediments of the Tibetan Tethys Himalaya in the area of Tingri (south Tibet), Rep. 38, Berichte, Fachbereich Geowissenschaften, Univ. Bremen, Bremen, Germany.
- Willems, H., et al. (1996), Stratigraphy of the Upper Cretaceous and lower Tertiary strata in the Tethyan Himalayas of Tibet (Tingri area, China), *Geol. Rundsch.*, *85*, 723–754, doi:10.1007/BF02440107.
- Zhang, H., et al. (2010), The significance of Cenozoic magmatism from the western margin of the eastern syntaxis, southeast Tibet, *Contrib. Mineral. Petrol.*, *160*, 83–98.
- Zhu, B. (2003), Sedimentology, petrography and tectonic significance of Cretaceous to lower Tertiary deposits in the Tingri-Gyangtse area, southern Tibet., Ph.D. thesis, 213 pp., State Univ. of New York at Albany, Albany, N. Y.
- Zhu, B., et al. (2005), Age of initiation of the India-Asia collision in the east-central Himalaya, *J. Geol.*, *113*, 265–285, doi:10.1086/428805.
- Zhu, B., et al. (2006), Age of initiation of the India-Asia collision in the east-central Himalaya: A reply, *J. Geol.*, *114*, 641–643, doi:10.1086/506167.
- E. Appel and U. Liebke, Institut für Geowissenschaften Sigwartstrasse, University of Tuebingen, Tuebingen D-72074, Germany.
- M. Boudagher-Fadel, P. Bown, and A. Carter, Department of Geological Sciences, UCL, London WC1E 6BT, UK.
- E. Garzanti and G. Vezzoli, Dipartimento di Scienze Geologiche e Geotecnologie, University of Milano-Bicocca, Milan I-20126, Italy.
- L. Godin, Department of Geological Sciences, Queen's University at Kingston, Kingston, ON K7L 3N6, Canada.
- J. Han, Department of Geology, CAS, Beijing 100864, China.
- Y. Najman, Lancaster Environment Centre, University of Lancaster, Lancaster LA1 4YQ, UK.
- G. Oliver, School of Geography and Geosciences, University of St Andrews, St Andrews KY16 9AJ, UK.
- R. Parrish, NIGL, BGS Keyworth, Nottingham NG12 5GG, UK.